

CERN-PH-EP/2013-084
2013/08/22

CMS-FSQ-12-010

Study of exclusive two-photon production of W^+W^- in pp collisions at $\sqrt{s} = 7$ TeV and constraints on anomalous quartic gauge couplings

The CMS Collaboration*

Abstract

A search for exclusive or quasi-exclusive W^+W^- production by photon-photon interactions, $pp \rightarrow p^{(*)}W^+W^-p^{(*)}$, at $\sqrt{s} = 7$ TeV is reported using data collected by the CMS detector with an integrated luminosity of 5.05 fb^{-1} . Events are selected by requiring a $\mu^\pm e^\mp$ vertex with no additional associated charged tracks and dilepton transverse momentum $p_T(\mu^\pm e^\mp) > 30 \text{ GeV}$. Two events passing all selection requirements are observed in the data, compared to a standard model expectation of 2.2 ± 0.4 signal events with 0.84 ± 0.15 background. The tail of the dilepton p_T distribution is studied for deviations from the standard model. No events are observed with $p_T > 100 \text{ GeV}$. Model-independent upper limits are computed and compared to predictions involving anomalous quartic gauge couplings. The limits on the parameters $a_{0,C}^W/\Lambda^2$ with a dipole form factor and an energy cutoff $\Lambda_{\text{cutoff}} = 500 \text{ GeV}$ are of the order of 10^{-4} .

Published in the Journal of High Energy Physics as doi:10.1007/JHEP07(2013)116.

1 Introduction

The detection of high-energy photon interactions at the Large Hadron Collider (LHC) opens up the possibility of interesting and novel research [1, 2]. In particular, measurements of the two-photon production of a pair of W -bosons provide sensitivity to anomalous quartic gauge couplings of the gauge bosons. Exploratory studies [3, 4] showed potential for extending the experimental reach by several orders of magnitude with respect to the best limits so far obtained at the Tevatron [5] and LEP [6–13]. First measurements of the exclusive two-photon production of muon and electron pairs at $\sqrt{s} = 7$ TeV, $pp \rightarrow p\ell^+\ell^-p$, were made using ~ 40 pb $^{-1}$ of data collected with the Compact Muon Solenoid (CMS) at the LHC in 2010 [14, 15]. The present analysis is based on the experimental technique developed in Ref. [14] and uses the full data sample collected by the CMS experiment in 2011.

In this analysis the $\mu^\pm e^\mp$ final state is used to search for fully exclusive (“elastic”) $pp \rightarrow pW^+W^-p$ production. Since both very forward-scattered protons escape detection, such a production process is characterized by a primary vertex formed from a $\mu^\pm e^\mp$ pair with no other tracks, with large transverse momentum, $p_T(\mu^\pm e^\mp)$, and large invariant mass, $m(\mu^\pm e^\mp)$. This signature is also accessible via quasi-exclusive (“inelastic” or “proton dissociative”) production, in which one or both of the incident protons dissociate into a low-mass system that escapes detection, denoted as p^* . The two-photon signal $\gamma\gamma \rightarrow W^+W^-$ is therefore comprised of both the elastic and inelastic contributions.

In the case of decays of the W^+W^- pair to same-flavor $\mu^+\mu^-$ or e^+e^- final states, the backgrounds are more than an order of magnitude larger than in the $\mu^\pm e^\mp$ final state. Therefore in the present analysis, only the $\mu^\pm e^\mp$ channel is used to search for a $pp \rightarrow p^{(*)}W^+W^-p^{(*)}$ signal. We use the $\mu^+\mu^-$ channel to select a control sample of high-mass $pp \rightarrow p^{(*)}\mu^+\mu^-p^{(*)}$ events originating mainly from direct $\gamma\gamma \rightarrow \mu^+\mu^-$ production. Final states containing a $\mu^\pm e^\mp$ pair may arise from direct decays of W^\pm bosons to electrons and muons or from $W \rightarrow \tau\nu$ decays, with the τ subsequently decaying to an electron or a muon. For brevity, we will refer to the full reaction as $pp \rightarrow p^{(*)}W^+W^-p^{(*)} \rightarrow p^{(*)}\mu^\pm e^\mp p^{(*)}$, where the final state is understood to contain between two and four undetected neutrinos, in addition to the charged $\mu^\pm e^\mp$ pair.

We first use the $pp \rightarrow p^{(*)}\mu^+\mu^-p^{(*)}$ control sample to validate the selection by comparing the expected and observed numbers of events and to estimate from the data the proton dissociative contribution. The dominant backgrounds in the $\mu^\pm e^\mp$ channel, due to the inclusive production of W^+W^- and $\tau^+\tau^-$ pairs, are then constrained using control regions with low $p_T(\mu^\pm e^\mp)$ or a low-multiplicity requirement for extra tracks originating from the $\mu^\pm e^\mp$ vertex.

The data for the signal region are then compared to the standard model (SM) expectation for the backgrounds and the $\gamma\gamma \rightarrow W^+W^-$ signal. Finally, tails of the $p_T(\mu^\pm e^\mp)$ distribution, where the SM $\gamma\gamma \rightarrow W^+W^-$ contribution is expected to be small, are investigated to look for anomalous quartic gauge couplings [16].

The paper is organized as follows. Section 2 describes the CMS detector. Section 3 presents the theory related to the $\gamma\gamma \rightarrow W^+W^-$ process and the approach to deal with the anomalous couplings, together with the description of the simulated data. In Section 4 the trigger, lepton identification, and preselection criteria employed in this analysis are presented in detail. The study of the $pp \rightarrow p^{(*)}\mu^+\mu^-p^{(*)}$ control sample is discussed in Section 5, while the investigation of the $\mu^\pm e^\mp$ signal for the elastic and proton dissociative W^+W^- production is presented in Section 6. Next, Section 7 describes the impact of the systematic uncertainties encountered in this analysis along with the additional checks for the background modelling. Finally, the results of this analysis are presented in Section 8, followed by the summary in Section 9.

2 The CMS detector

A detailed description of the CMS experiment can be found elsewhere [17]. The central feature of the CMS apparatus is a superconducting solenoid, of 6 m internal diameter. Within the field volume are the silicon pixel and strip tracker, the crystal electromagnetic calorimeter (ECAL), and the brass-scintillator hadron calorimeter (HCAL). Muons are measured in gas-ionization detectors embedded in the steel flux-return yoke of the magnet. Besides the barrel and endcap detectors, CMS has extensive forward calorimetry.

The CMS experiment uses a right-handed coordinate system, with the origin at the nominal collision point, the x axis pointing towards the center of the LHC ring, the y axis pointing up (perpendicular to the plane of LHC ring), and the z axis along the anticlockwise-beam direction. The polar angle θ is measured from the positive z axis and the azimuthal angle ϕ is measured, in radians, in the (x, y) plane relative to the x axis. The silicon tracker covers a range of $|\eta| < 2.4$, where $\eta = -\ln[\tan(\theta/2)]$, and consists of three layers made of 66 million $100 \times 150 \mu\text{m}^2$ pixels followed by ten microstrip layers, with strips of pitch between 80 and $180 \mu\text{m}$. Muons are measured in the $|\eta| < 2.4$ range, with detection planes made of three technologies: drift tubes, cathode strip chambers, and resistive-plate chambers. The 3.8 T magnetic field, and the high granularity of the silicon tracker, allow the transverse momentum of the muons matched to tracks in the silicon detector to be measured with a resolution better than $\sim 1.5\%$ for p_T smaller than 100 GeV. The ECAL provides coverage in a range of $|\eta| < 1.479$ in the barrel region and $1.479 < |\eta| < 3.0$ in the two endcap regions. The first level of the CMS trigger system, composed of custom hardware processors, uses information from the calorimeters and muon detectors to select (in less than $3 \mu\text{s}$) the most interesting events. The high-level trigger (HLT) processor farm further decreases the event rate from 100 kHz to a few hundred Hz before data storage.

3 Theory and simulation

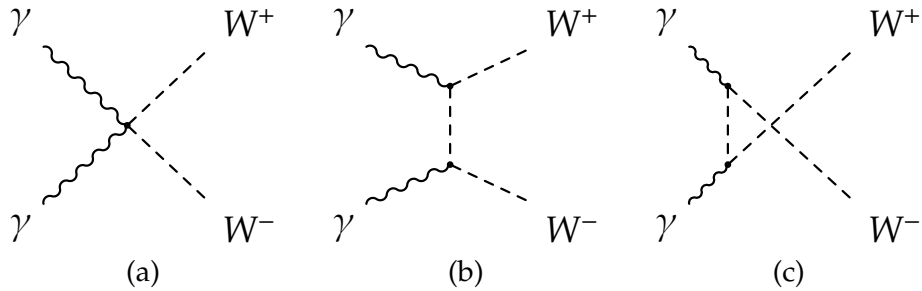


Figure 1: Quartic gauge coupling (a) and t - (b) and u -channel (c) W -boson exchange diagrams contributing to the $\gamma\gamma \rightarrow W^+W^-$ process at leading order in the SM.

The electroweak sector of the SM [18–20] predicts 3- and 4-point vertices with the gauge bosons, which are represented in the SM Lagrangian by the following terms for the quartic $WW\gamma\gamma$ and triple $WW\gamma$ couplings:

$$\begin{aligned} L^{WW\gamma} &= -ie (\partial_\mu A_\nu - \partial_\nu A_\mu) W^{+\mu} W^{-\nu} \\ L^{WW\gamma\gamma} &= -e^2 (W_\mu^+ W^{-\mu} A_\nu A^\nu - W_\mu^+ W_\nu^- A^\mu A^\nu) \end{aligned} \quad (1)$$

where A^μ is the photon field and W^μ is the W -boson field. As a result, the diagrams that represent the $WW\gamma\gamma$ interaction at lowest order in the perturbation series consist of both quartic gauge coupling (Fig. 1(a)) and t - and u -channel W -boson exchange diagrams (Fig. 1(b,c)).

Measurements of the quartic $WW\gamma\gamma$ coupling can be used to look for any deviation from the SM predictions, which would reveal a sign of new physics [6]. One has to take into account more generic couplings in order to study the possibility of such deviations in high-energy collisions. Considering models with the anomalous triple gauge couplings, the quartic $WW\gamma\gamma$ and triple $WW\gamma$ couplings can be associated with a single anomalous dimension-six operator [16]. The genuine anomalous quartic gauge couplings considered here are instead introduced via an effective Lagrangian containing new terms respecting local $U(1)_{\text{EM}}$ and global custodial $SU(2)_C$ symmetry. Further imposing charge-conjugation and parity symmetries, C - and P -, results in a minimum of two additional dimension-six terms, containing the parameters a_0^W and a_C^W [16]:

$$\begin{aligned} L_6^0 &= \frac{e^2}{8} \frac{a_0^W}{\Lambda^2} F_{\mu\nu} F^{\mu\nu} W^{+\alpha} W_\alpha^- - \frac{e^2}{16 \cos^2 \Theta_W} \frac{a_0^Z}{\Lambda^2} F_{\mu\nu} F^{\mu\nu} Z^\alpha Z_\alpha \\ L_6^C &= \frac{-e^2}{16} \frac{a_C^W}{\Lambda^2} F_{\mu\alpha} F^{\mu\beta} (W^{+\alpha} W_\beta^- + W^{-\alpha} W_\beta^+) - \frac{e^2}{16 \cos^2 \Theta_W} \frac{a_C^Z}{\Lambda^2} F_{\mu\alpha} F^{\mu\beta} Z^\alpha Z_\beta \end{aligned} \quad (2)$$

where Λ_{cutoff} is the energy cutoff scale for the form factor and the second terms in the expressions are those corresponding to the Z-boson couplings. These genuine anomalous quartic couplings are therefore completely independent of the SM triple and quartic gauge couplings. While the $\gamma\gamma \rightarrow W^+W^-$ process contains two triple gauge coupling vertices involving t-channel W-boson exchange (Fig. 1 left), the sensitivity to anomalous triple gauge couplings is not expected to significantly surpass the existing experimental limits on $WW\gamma$ couplings from single triple gauge coupling processes [4]. Hence, only anomalous quartic gauge couplings are considered in the analysis, assuming no anomalous triple gauge couplings are present.

The existing constraints on anomalous quartic gauge couplings from e^+e^- collisions at LEP are derived from $e^+e^- \rightarrow W^+W^-\gamma$ and $W^+W^- \rightarrow \gamma\gamma$ interactions in which the effective center-of-mass energy is limited to values well below the e^+e^- center-of-mass energy of $\sqrt{s} = 209$ GeV. In contrast, the spectrum of $\gamma\gamma$ interactions at the LHC and the Tevatron extends to much higher values, resulting in increased sensitivity to anomalous couplings.

The $\gamma\gamma \rightarrow W^+W^-$ cross section increases quadratically with anomalous coupling strength, and consequently unitarity is violated for high-energy $\gamma\gamma$ interactions. For anomalous couplings a_0^W/Λ^2 , a_C^W/Λ^2 of order 10^{-5} , the unitarity bound is already reached for collisions with a $\gamma\gamma$ center-of-mass energy $W_{\gamma\gamma} \sim 1$ TeV [3, 4]. In order to tame this rising of the cross section, both a_0^W/Λ^2 and a_C^W/Λ^2 parameters are multiplied by a form factor :

$$a_{0,C}^W(W_{\gamma\gamma}^2) = \frac{a_{0,C}^W}{\left(1 + \frac{W_{\gamma\gamma}^2}{\Lambda_{\text{cutoff}}^2}\right)^p}$$

where p is a free parameter, which is conventionally set to 2 (dipole form factor), following previous studies of anomalous quartic gauge couplings [21, 22]. Because the new physics that enters to regulate the cross section has an energy scale Λ and a form that are a priori unknown, we consider both a scenario with a dipole form factor with energy cutoff scale $\Lambda_{\text{cutoff}} = 500$ GeV, and a scenario with no form factor (i.e., $\Lambda_{\text{cutoff}} \rightarrow \infty$).

The $\gamma\gamma \rightarrow W^+W^-$ signal is generated using CALCHEP2.5.4 [23], with PYTHIA6.422 [24] used to simulate the decay of the W^+W^- pair. The simulated inclusive background samples used in this analysis are produced with MADGRAPH5 [25] for $W^+W^- + \text{jets}$, $W + \text{jets}$, and $t\bar{t}$ processes, and with POWHEG 1.0 [24, 26–28] for $\tau^+\tau^-$ pairs produced via the Drell–Yan process. In the simulated $W^+W^- + \text{jets}$, $W + \text{jets}$, $t\bar{t}$, and Drell–Yan background samples, τ -decays are handled

by the TAUOLA [29] package. Inclusive W^+W^- production at the LHC is expected to be dominated by s -channel and t -channel $q\bar{q} \rightarrow W^+W^-$ interactions, followed by a small ($\sim 3\%$) contribution from gluon-gluon interactions [30]. This inclusive W^+W^- background sample is scaled to the next-to-leading-order (NLO) prediction obtained from MCFM [31], which describes the experimentally measured cross section [32, 33] within the uncertainties. The underlying event in all background processes is simulated using the Z2 tune [34] of PYTHIA.

In addition to the inclusive W^+W^- backgrounds, we consider W^+W^- production from single diffractive interactions, and from $WW \rightarrow WW$ scattering (vector boson fusion). The diffractive W^+W^- background is generated using POMPYT [35]. Single diffractive W^+W^- production will result in events with a multiplicity of extra tracks lower than that of non-diffractive production, and with large theoretical uncertainties related to survival probabilities that will suppress the visible cross section. We conservatively consider the diffractive W^+W^- background with no survival probability correction in the default background estimate. The two-photon processes, $\gamma\gamma \rightarrow \mu^+\mu^-$ and $\gamma\gamma \rightarrow \tau^+\tau^-$, are produced using LPAIR [36, 37], which describes well the exclusive and quasi-exclusive dilepton measurements of CMS [14, 15]. The contribution from (gluon-mediated) central exclusive W^+W^- production is estimated to be $\lesssim 1\%$ of the $\gamma\gamma \rightarrow W^+W^-$ cross section [38] and is neglected in the current analysis. The VBFNLO generator [39] is used to study backgrounds from $WW \rightarrow WW$ scattering, with PYTHIA used for hadronization and the decay of the W^+W^- pair. All signal and background samples are produced with a detailed GEANT4 [40] simulation of the CMS detector.

4 Event selection

The data used in this analysis correspond to the full sample collected in 2011 at $\sqrt{s} = 7$ TeV with the CMS detector. In the $\mu^\pm e^\mp$ channel all detector subsystems are required to pass the standard data quality requirements, resulting in a sample with an integrated luminosity of 5.05 fb^{-1} . In the $\mu^+\mu^-$ channel, which is used only as a control sample, a less restrictive selection is used, requiring that only the muon or tracking systems pass the data quality requirements. This results in a sample with a slightly higher integrated luminosity of 5.24 fb^{-1} .

In the $\mu^\pm e^\mp$ channel events are selected online by two electron-muon HLT algorithms with asymmetric thresholds. The first algorithm requires a muon of 17 GeV and an electron of 8 GeV, while the second requires a muon of 8 GeV and an electron of 17 GeV. In the $\mu^\pm\mu^\mp$ channel, dimuon triggers with asymmetric 17 GeV and 8 GeV thresholds on the two muons are used for consistency with the $\mu^\pm e^\mp$ channel.

Muon candidates are required to pass a tight muon selection similar to that described in detail in Ref. [14]. Electrons are required to pass a medium identification selection with criteria chosen to ensure the offline selection is tighter than the trigger requirement. The electron selection is similar to that of Ref. [41] and includes requirements on the shower shape measured in the ECAL, the transverse and longitudinal impact parameters with respect to the primary vertex, an isolation criterion based on combined information from the silicon tracker and calorimeters, the number of missing hits on the electron track, and the incompatibility of the electron and nearby tracks with those originating from a photon conversion. A particle flow (PF) algorithm [42] is used to reconstruct particles in the event by combining information from all detector systems. The missing transverse energy \cancel{E}_T is then computed from the negative vector sum of all particles.

After trigger selection and lepton identification, a first preselection criterion is applied offline on the data by requiring a reconstructed muon and electron of opposite charge, each having

$p_T > 20 \text{ GeV}$ and $|\eta| < 2.4$, matched to a common primary vertex with fewer than 15 additional tracks. After the trigger selection, the leptons are required to have an invariant mass $m(\ell^+ \ell'^-) > 20 \text{ GeV}$ in both the $\mu^\pm e^\mp$ and $\mu^+ \mu^-$ channels. In the remainder of this paper we will use the notation $p_T(\ell^+, \ell'^-)$ to indicate a p_T selection applied to each lepton of the pair, and $p_T(\ell^+ \ell'^-)$ to indicate the p_T of the pair.

At high luminosities, almost all signal events will have additional interactions within the same bunch crossing (“pileup”), that produce extra charged tracks and extra activity in the calorimeters. During the 2011 LHC run the average number of interactions per crossing was approximately 9. In order to retain efficiency in high pileup conditions, a selection based only on the number of charged tracks originating from the same primary vertex as the $\ell^+ \ell'^-$ pair is used, similar to the method in Ref. [14].

In the $\mu^\pm e^\mp$ channel the SM signal region is defined to have zero extra tracks associated with the $\mu^\pm e^\mp$ vertex, and transverse momentum of the pair $p_T(\mu^\pm e^\mp) > 30 \text{ GeV}$. The first requirement rejects backgrounds from inclusive production, while the second is chosen based on the simulated $p_T(\mu^\pm e^\mp)$ distribution of the signal and $\tau^+ \tau^-$ background events. The efficiency for reconstruction of primary vertices with two or more tracks has been measured to be $\geq 98\%$ in simulation, and $\geq 99\%$ in data. In addition, events are only accepted as $\mu^\pm e^\mp$ events if they have failed to satisfy the $\mu^\pm \mu^\mp$ selection, in order to reject $\gamma\gamma \rightarrow \mu^+ \mu^-$ events with the muon misidentified as an electron due to a bremsstrahlung photon overlapping with the muon track.

For the anomalous quartic gauge couplings search, a restricted region of $p_T(\mu^\pm e^\mp) > 100 \text{ GeV}$ is used. This is chosen to reduce the expected SM $\gamma\gamma \rightarrow W^+ W^-$ contribution to approximately 0.1 events after all selection requirements, while retaining sensitivity to anomalous couplings of order 10^{-4} for $\Lambda_{\text{cutoff}} = 500 \text{ GeV}$ or larger (Fig. 2). This corresponds to values of the anomalous quartic gauge coupling parameters approximately two orders of magnitude smaller than the limits obtained at LEP [8, 11, 13] and approximately one order of magnitude smaller than Tevatron limits [5].

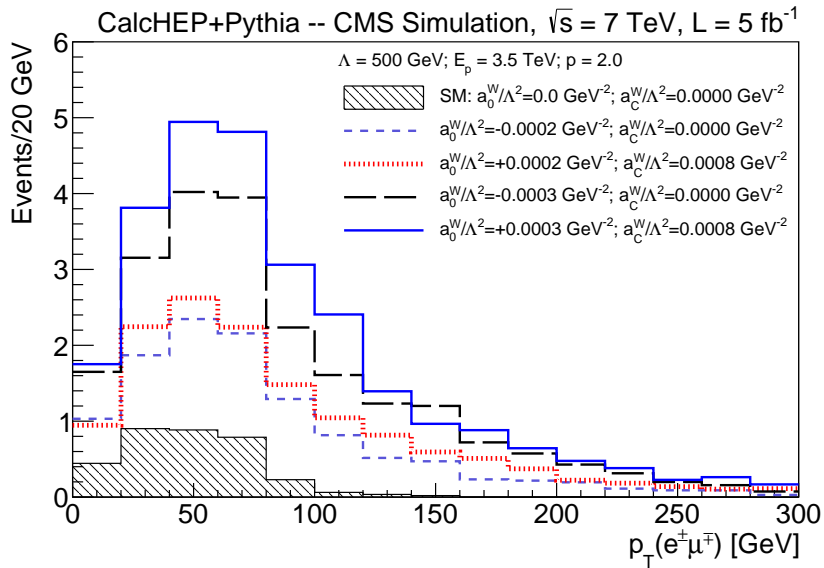


Figure 2: Transverse momentum distribution of lepton pairs for the $\gamma\gamma \rightarrow W^+ W^-$ process at generator level in the SM (shaded histogram), and for several values of anomalous quartic gauge coupling parameters a_0^W and a_C^W (open histograms). In this plot $\Lambda_{\text{cutoff}} = 500 \text{ GeV}$ is the energy cutoff scale in the dipole form factor.

5 Cross checks with $\mu^+\mu^-$ events

In the case of same-flavor dilepton final states, the background due to Drell–Yan ($pp \rightarrow \ell^\pm \ell^\mp X$) or $pp \rightarrow p^{(*)} \ell^\pm \ell^\mp p^{(*)}$ production is more than an order of magnitude larger than the unlike-flavor $\mu^\pm e^\mp$ channel of the $\gamma\gamma \rightarrow W^+W^-$ signal for the same selection criteria. The semileptonic and fully hadronic channels, in which one or both W s decay into a $q\bar{q}$ pair, are similarly dominated by background and complicated by the requirement of matching the constituents of the resulting jets to the primary vertex. As a test benchmark for high-mass lepton pair detection, elastic $\gamma\gamma \rightarrow \mu^+\mu^-$ production is used because of the small theoretical uncertainties on the cross section [36].

The dimuon sample with zero extra tracks is divided into two kinematic regions based on the p_T balance ($|\Delta p_T(\mu^+\mu^-)|$) and acoplanarity ($1 - |\Delta\phi(\mu^+\mu^-)/\pi|$) of the pair. The first region with $1 - |\Delta\phi(\mu^+\mu^-)/\pi| < 0.1$ and $|\Delta p_T(\mu^+\mu^-)| < 1 \text{ GeV}$ is defined as the “elastic” region, where the dimuon kinematic requirements are consistent with elastic $pp \rightarrow p\mu^+\mu^-p$ events where both protons remain intact [14]. The second region with $1 - |\Delta\phi(\mu^+\mu^-)/\pi| > 0.1$ or $|\Delta p_T(\mu^+\mu^-)| > 1 \text{ GeV}$ (“dissociation” selection) is dominated by $\gamma\gamma \rightarrow \mu^+\mu^-$ interactions in which one or both protons dissociate. The latter process is less well-known theoretically, and subject to corrections from rescattering, in which strong interactions between the protons produce additional hadronic activity. As this effect is not included in the simulation, it may lead to a significant over-estimate of the proton dissociation contribution in two-photon interactions [43]. We therefore use this second control region to estimate the proton dissociation yield directly from data.

The contributions from exclusive Z production are expected to be negligible compared to the cross section of approximately 0.5 pb from $\gamma\gamma \rightarrow \mu^+\mu^-$, with $p_T(\mu^+, \mu^-) > 20 \text{ GeV}$. Exclusive Z photoproduction, $\gamma p \rightarrow Zp$, is expected to have a cross section smaller than 1 fb after taking into account the branching fraction to $\mu^+\mu^-$ [44–46], while the $\gamma\gamma \rightarrow Z$ process is forbidden at tree level. The Z -boson peak therefore provides another cross-check of the residual inclusive Drell–Yan contamination in both regions. In Fig. 3 the invariant mass distribution in the elastic-enhanced region is shown, with the marked Z -peak region defined as $70 \text{ GeV} < m(\mu^+\mu^-) < 106 \text{ GeV}$. In Fig. 4 the dimuon kinematic distributions for events having zero extra tracks are shown. The distributions are plotted separately for the Z -peak region, which is expected to include a large inclusive Drell–Yan component, and for the region outside the Z peak, which is expected to be dominated by two-photon interactions. For the kinematic distributions with zero extra tracks originating from the $\mu^+\mu^-$ production vertex, good agreement is observed between data and simulation. This confirms that pileup effects and low-multiplicity fluctuations of the inclusive Drell–Yan processes are well modeled. The hatched bands indicate the statistical uncertainty. In Fig. 5 the dimuon pair invariant mass is plotted for the dissociation selection with zero extra tracks.

Table 1 lists the number of events with zero extra tracks seen in the data and expected from simulation in the $\mu^+\mu^-$ sample after trigger and preselection criteria. In the elastic region, the sum of all contributions in simulation using the LPAIR generator is $\sim 10\%$ greater than the yield observed in data. In the dissociation region, which is expected to be most affected by rescattering corrections [43], an overall deficit of 28% is observed in the data. As seen in Fig. 6, this deficit is particularly large at high $p_T(\mu^+\mu^-)$.

The suppression due to rescattering corrections is particularly significant in the case of quasi-exclusive production when one or both incident protons dissociate. This suppression is practically impossible to calculate from first principles as it involves very soft interactions and only phenomenological models are available. Therefore, using the low-background sample

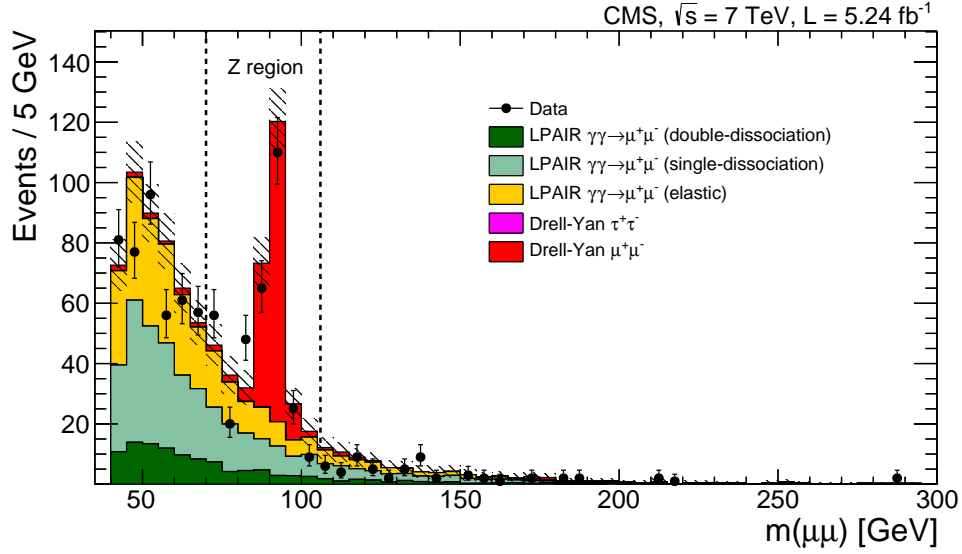


Figure 3: Invariant mass distribution of the muon pairs for the elastic selection with no additional track on the dimuon vertex. The dashed lines indicate the Z-peak region. The hatched bands indicate the statistical uncertainty in the simulation.

Table 1: Total number of data events compared to the sum of all the background events expected in the two control regions, after trigger and preselection criteria. The uncertainties are statistical only.

Region	Data	Simulation	Data/Simulation
Elastic	820	906 ± 9	0.91 ± 0.03
Dissociation	1312	1830 ± 17	0.72 ± 0.02
Total	2132	2736 ± 19	0.78 ± 0.02

of dimuons produced via two-photon interactions, we use the data to determine an effective, observed “luminosity” of two-photon interactions at high energies relevant for W -pair production. For this purpose, the number of detected dimuon events with invariant mass over 160 GeV, corrected for the DY contribution, is divided by the prediction for the fully exclusive, elastic production predicted by LPAIR,

$$F = \frac{N_{\mu\mu \text{ data}} - N_{\text{DY}}}{N_{\text{elastic}}} \Big|_{m(\mu^+\mu^-) > 160 \text{ GeV}} \quad (3)$$

$$F = 3.23 \pm 0.53.$$

This factor F is then be applied to scale the CALCHEP signal prediction and obtain the total cross section for two-photon W^+W^- production including elastic and proton dissociative contributions. This assumes the dilepton kinematics are the same in elastic and proton dissociative production, with the difference in efficiency arising from the requirement of zero extra tracks originating from the W^+W^- production vertex.

A total uncertainty of 16% on this factor F is assigned, which has two independent sources. The first source is a 15.5% statistical uncertainty in the determination of this factor from the high-mass dimuon data. The second source is due to applying the scale factor derived from the matrix-element LPAIR generator to the $\gamma\gamma \rightarrow W^+W^-$ signal sample produced with CALCHEP according to the equivalent photon approximation (EPA) [47]. This is checked by comparing the LPAIR prediction with the EPA prediction for muon pair production above 160 GeV in in-

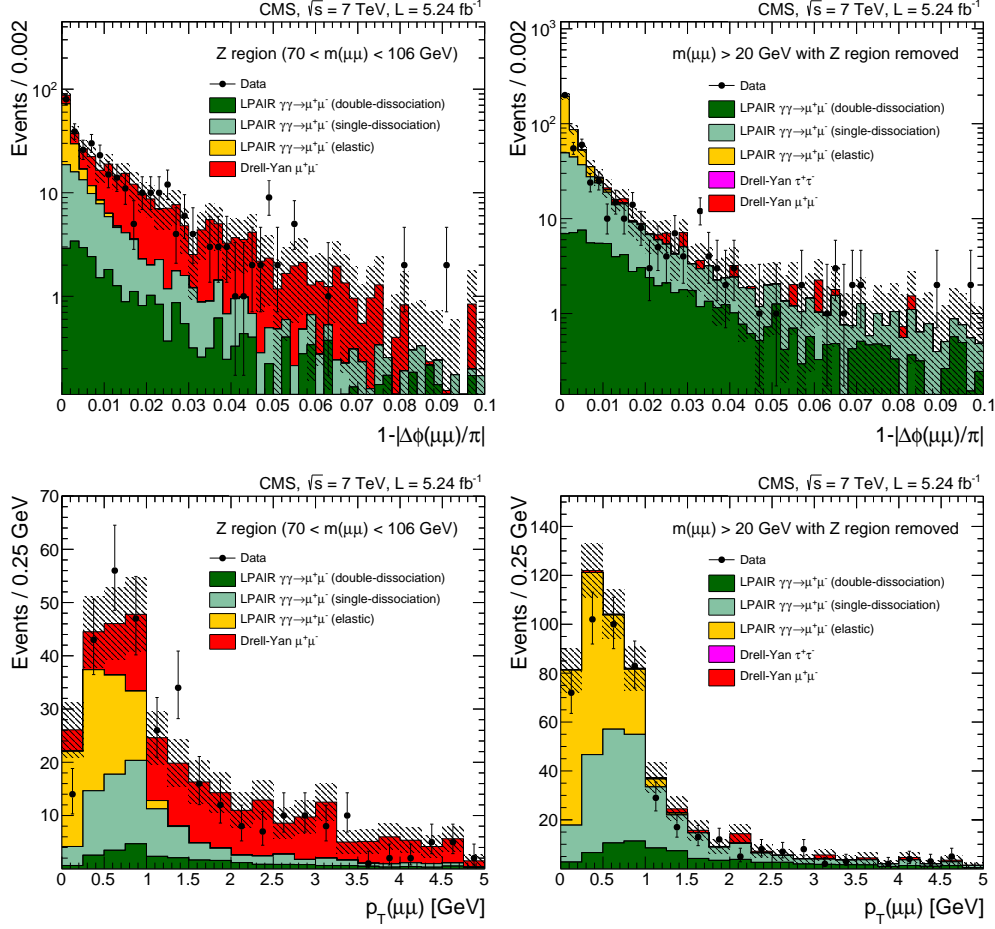


Figure 4: Kinematic distributions for the elastic selection, for the Z region only ($70\text{ GeV} < m(\mu^+\mu^-) < 106\text{ GeV}$, left panel) and with the Z region removed (right panel). The acoplanarity (above) and p_T of $\mu^+\mu^-$ pairs with zero extra tracks (below) are shown. The hatched bands indicate the statistical uncertainty in the simulation.

variant mass, and is taken conservatively as 5%.

6 The $W^+W^- \rightarrow \mu^\pm e^\mp$ signal

The SM cross section for the purely elastic process $pp \rightarrow pW^+W^-p$ is predicted to be 40.0 fb using CALCHEP, or 1.2 fb for the cross section times branching fraction to $\mu^\pm e^\mp$ final states [48]. Using the scale factor F extracted from the high-mass $\gamma\gamma \rightarrow \mu^+\mu^-$ sample to account for the additional proton dissociation contribution, the total predicted cross section times branching fraction is:

$$\sigma_{\text{theory}}(pp \rightarrow p^{(*)}W^+W^-p^{(*)} \rightarrow p^{(*)}\mu^\pm e^\mp p^{(*)}) = 4.0 \pm 0.7\text{ fb}.$$

The acceptance for the SM signal in the fiducial region $|\eta(\mu, e)| < 2.4$, $p_T(\mu, e) > 20\text{ GeV}$ is determined to be 55% using the CALCHEP generator.

The predicted visible cross section at each stage of the selection, defined as the predicted cross section multiplied by the efficiency and acceptance, is shown in Table 2, together with the efficiency and acceptance for the signal, and the corresponding number of events selected from the data sample. The signal inefficiency introduced by the requirement of zero extra tracks on the $\mu^\pm e^\mp$ vertex reflects the effect of pileup. As described in Ref. [14], with increasing pileup

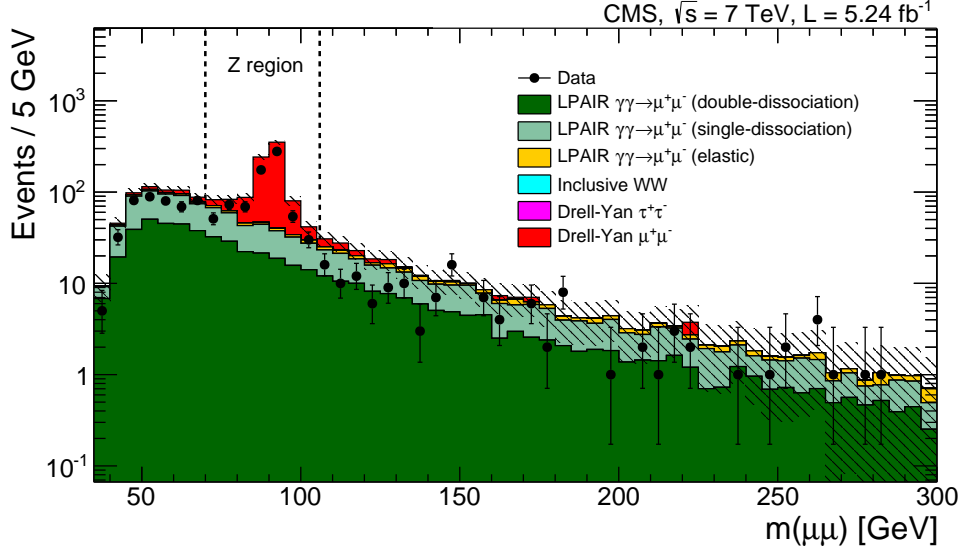


Figure 5: Invariant mass distribution of the muon pairs for the dissociation selection. The dashed lines indicate the Z-peak region. The hatched bands indicate the statistical uncertainty in the simulation.

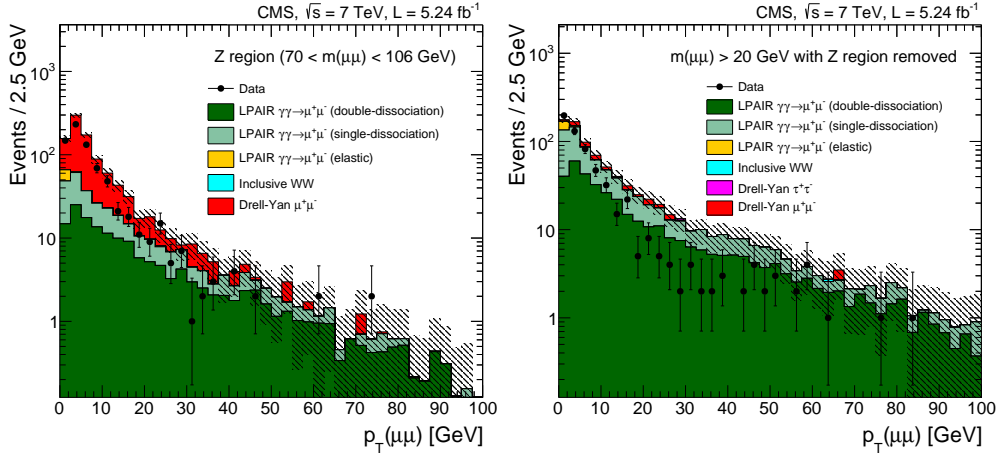


Figure 6: Transverse momentum distribution for $\mu^+\mu^-$ pairs with zero extra tracks passing the dissociation selection, for the Z region only (left), and with the Z region removed (right). The hatched bands indicate the statistical uncertainty in the simulation.

there is a higher probability of finding tracks from a pileup interaction in close proximity to the dilepton signal vertex. The incorrect assignment of these tracks to the signal vertex by the vertex clustering algorithm will lead to signal events being rejected. In the 2011 data sample with an average of 9 interactions per bunch crossing, this results in the rejection of $\sim 40\%$ of signal events that would pass other selection requirements.

To check the modelling of the individual background contributions, we define three independent control regions based on the number of tracks associated to the $\mu^\pm e^\mp$ vertex and the p_T of the $\mu^\pm e^\mp$ pair, as defined in Table 3. To study the inclusive backgrounds, we select two control regions with 1–6 extra tracks associated to the $\mu^\pm e^\mp$ vertex. The first region has $p_T(\mu^\pm e^\mp) < 30$ GeV and is dominated by inclusive Drell–Yan production of $\tau^+\tau^-$ and the second, with $p_T(\mu^\pm e^\mp) > 30$ GeV, is dominated by inclusive W^+W^- production. In order to select a sample with a significant fraction of $\gamma\gamma \rightarrow \tau^+\tau^-$ events, we define a third control region having zero extra tracks, but $p_T(\mu^\pm e^\mp) < 30$ GeV.

Table 2: Product of the signal efficiency and the acceptance, visible cross section, and number of events selected in data at each stage of the selection. The preselection requires a reconstructed muon and electron of opposite charge, each having $p_T > 20$ GeV and $|\eta| < 2.4$, matched to a common primary vertex with fewer than 15 additional tracks.

Selection step	Signal $\epsilon \times A$	Visible cross section (fb)	Events in data
Trigger and preselection	28.5%	1.1	9086
$m(\mu^\pm e^\mp) > 20$ GeV	28.0%	1.1	8200
Muon ID and Electron ID	22.6%	0.9	1222
$\mu^\pm e^\mp$ vertex with zero extra tracks	13.7%	0.6	6
$p_T(\mu^\pm e^\mp) > 30$ GeV	10.6%	0.4	2

Table 3: Definitions for the three independent control regions.

Region	Background process	$N_{\text{extra tracks}}$	$p_T(\mu^\pm e^\mp)$
1	Inclusive W^+W^-	$1 \leq N_{\text{extra tracks}} \leq 6$	> 30 GeV
2	Inclusive Drell–Yan $\tau^+\tau^-$	$1 \leq N_{\text{extra tracks}} \leq 6$	< 30 GeV
3	$\gamma\gamma \rightarrow \tau^+\tau^-$	$N_{\text{extra tracks}} = 0$	< 30 GeV

We first compare the data to the expected backgrounds from simulation in the inclusive W^+W^- region. The predicted POMPYT diffractive W^+W^- contribution is, very conservatively, added to the other backgrounds, without accounting for any survival probabilities or overlap with the inclusive W^+W^- sample. To study the $W + \text{jets}$ backgrounds, for which the contribution is mainly from misidentified leptons or non-prompt leptons in jets, we select a control sample of events with $p_T(\mu^\pm e^\mp) > 30$ GeV, where at least one of the two lepton candidates fails the nominal offline identification criteria. This sample is then normalized to the simulation in the high-multiplicity (more than 6 extra tracks) region and used to estimate the $W + \text{jets}$ background in the signal and inclusive W^+W^- control regions. Figure 7 shows the distribution of the number of extra tracks for the W^+W^- region with $p_T(\mu^\pm e^\mp) > 30$ GeV, together with the invariant mass and acoplanarity of the events with 1–6 extra tracks. In general the data are consistent with the sum of simulated backgrounds in this region.

In the Drell–Yan $\tau^+\tau^-$ -dominated region with $p_T(\mu^\pm e^\mp) < 30$ GeV and 1–6 tracks we find general agreement in the dilepton kinematic distributions, but an overall deficit in the data sample compared to simulation, with 256.7 ± 10.1 background events expected and 182 observed. Figure 8 shows the distribution of the number of extra tracks for the events with $p_T(\mu^\pm e^\mp) < 30$ GeV, together with the invariant mass and acoplanarity of the events with 1–6 extra tracks.

In the $\tau^+\tau^-$ sample with zero extra tracks, we find four events in the data sample, compared to a background expectation of 2.5 events from simulation, plus 0.9 events from the $\gamma\gamma \rightarrow W^+W^-$ signal. The expected contribution to the background from $\gamma\gamma \rightarrow \tau^+\tau^-$ is approximately 0.7 events. The invariant mass and acoplanarity distributions are shown in Fig. 9.

Table 4 summarizes the observed and expected background event yields for the three independent control regions. Tracks from pileup vertices may be wrongly associated to the $\mu^\pm e^\mp$ vertex from a $\gamma\gamma \rightarrow W^+W^-$ event, resulting in signal events being classified as 1–6 tracks events. This signal contamination, as well as that from signal events with $p_T(\mu^\pm e^\mp) < 30$ GeV, is estimated from simulation to be approximately one event or less in any of the control regions.

We use the simulated background sample, corrected for trigger and lepton identification efficiencies, to estimate the backgrounds in the signal region. The $W + \text{jets}$ contribution to the background is estimated from the control sample of events with lepton identification inverted,

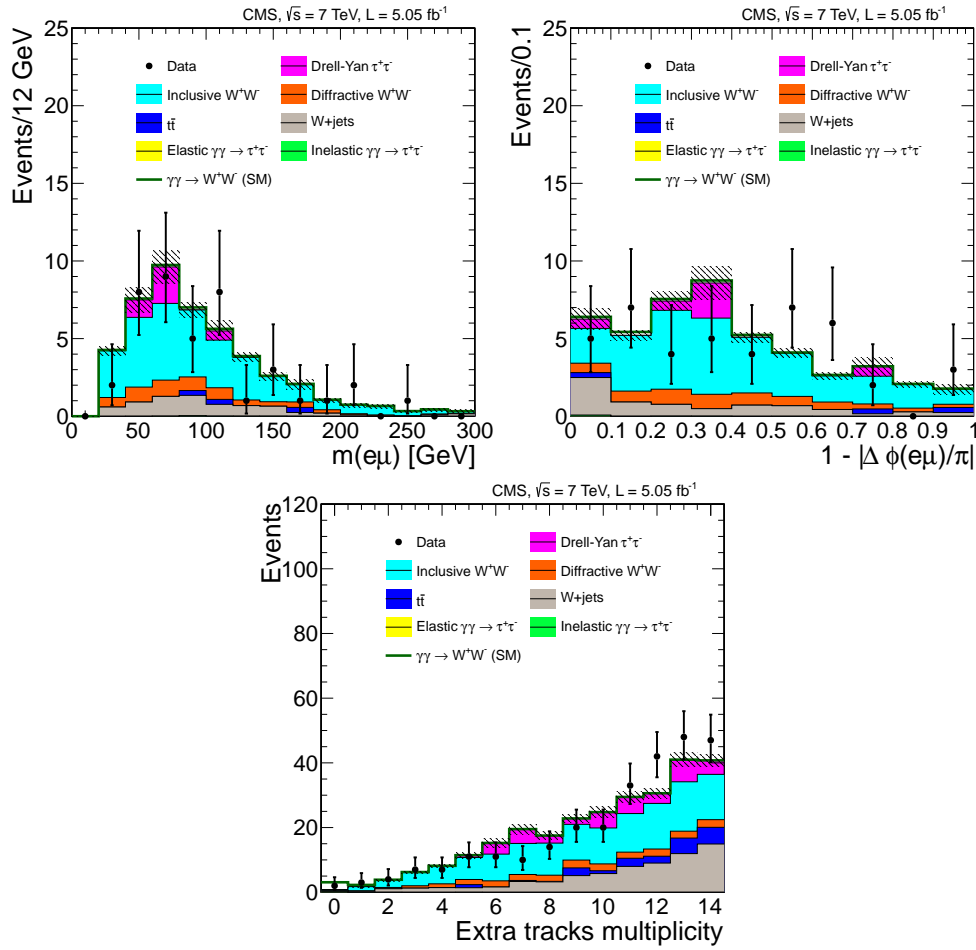


Figure 7: Data compared to simulation in control region 1. The $\mu^\pm e^\mp$ invariant mass (above left) and acoplanarity (above right) are shown for events with 1–6 extra tracks on the $\mu^\pm e^\mp$ vertex and $p_T(\mu^\pm e^\mp) > 30$ GeV. The number of additional tracks on the electron-muon primary vertex is shown for events with $p_T(\mu^\pm e^\mp) > 30$ GeV (below). The shaded bands indicate the statistical uncertainty in the background estimation. The signal (open histogram) is shown stacked on top of the backgrounds.

Table 4: Background event yields for the three independent control regions.

Region	Background process	Data	Sum of backgrounds	$\gamma\gamma \rightarrow W^+W^-$ signal
1	Inclusive W^+W^-	43	46.2 ± 1.7	1.0
2	Inclusive Drell-Yan $\tau^+\tau^-$	182	256.7 ± 10.1	0.3
3	$\gamma\gamma \rightarrow \tau^+\tau^-$	4	2.6 ± 0.8	0.7

while the $\gamma\gamma \rightarrow \tau^+\tau^-$ contribution is normalized using the factor derived from the high-mass $\gamma\gamma \rightarrow \mu^+\mu^-$ data sample. No simulated Drell-Yan $\tau^+\tau^-$ events survive all selection criteria, and a deficit of data compared to simulation is observed in the corresponding control region with 1–6 extra tracks and $p_T(\mu^\pm e^\mp) < 30$ GeV. Given this, and the agreement with data in the W^+W^- control region with 1–6 extra tracks and the $\tau^+\tau^-$ region with zero extra tracks, no additional rescaling of the backgrounds is performed. The estimated background is 0.84 ± 0.15 events, including the systematic uncertainty on the backgrounds.

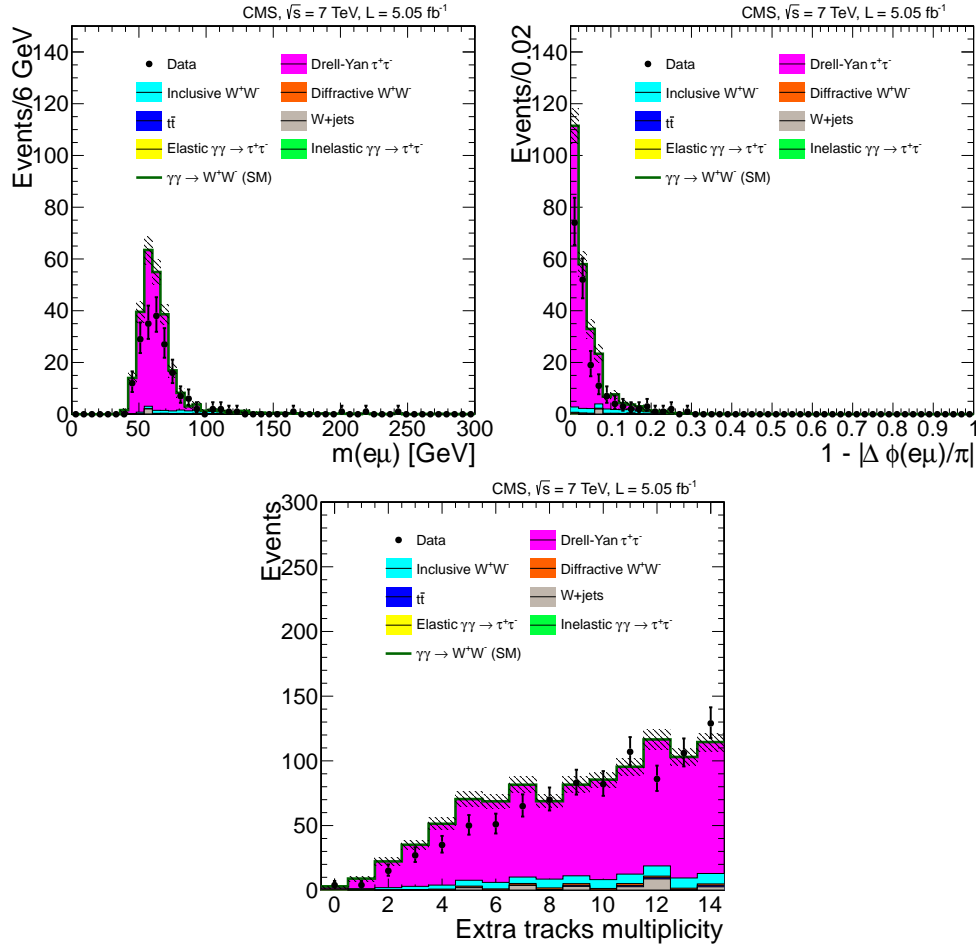


Figure 8: Data compared to simulation in control region 2. The $\mu^\pm e^\mp$ invariant mass (above left) and acoplanarity (above right) are shown for events with 1–6 extra tracks on the $\mu^\pm e^\mp$ vertex and $p_T(\mu^\pm e^\mp) < 30$ GeV. The number of additional tracks on the electron-muon primary vertex is shown for events with $p_T(\mu^\pm e^\mp) < 30$ GeV (below). The shaded bands indicate the statistical uncertainty in the background estimation. The signal (open histogram) is shown stacked on top of the backgrounds.

7 Systematics and cross-checks

The systematic uncertainties affecting the signal are summarized in Table 5. The uncertainty on the delivered 2011 luminosity is 2.2% [49]. The lepton trigger and selection efficiency corrections are varied by their $\pm 1\sigma$ statistical uncertainties, with the direction of the variation within each p_T and η bin correlated. The largest variation in the expected signal (when varying the efficiency scale factors by $+1\sigma$) is 4.2%, which is taken as a systematic uncertainty on the signal yield. The variation in the sum of backgrounds expected from simulation due to the trigger and lepton selection is 3.7%, which is taken as a component of the systematic uncertainty on the background estimate. The uncertainty on the efficiency for reconstructing vertices with two tracks is estimated to be 1.0%, based on the data vs. simulation difference obtained from the method described in Ref. [50].

The efficiency of the exclusivity selection, including effects from pileup, is checked using the $\gamma\gamma \rightarrow \mu^+\mu^-$ control sample. Using the elastic control region, where the theoretical uncertainties are smallest, we assign a 10% systematic uncertainty based on the level of agreement between data and simulation. In addition, we check the stability of the agreement between data and simulation as a function of pileup, using samples ranging from a minimum of 1-5

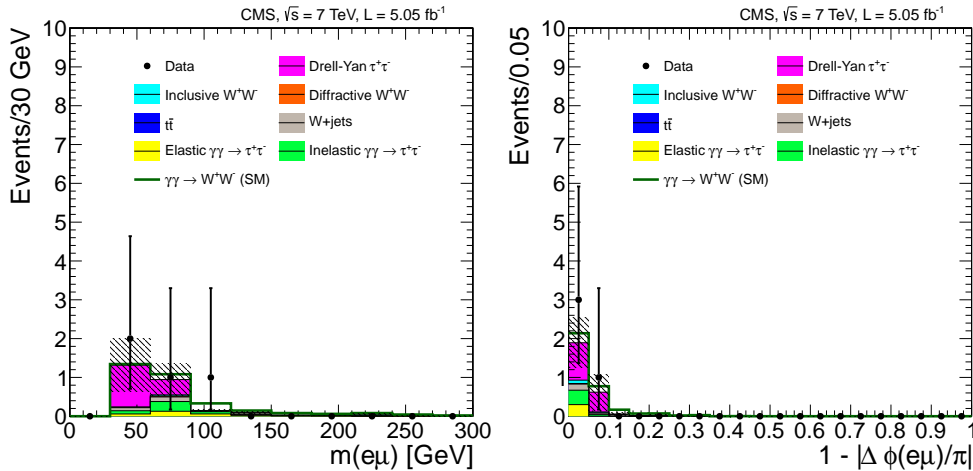


Figure 9: Data compared to simulation for control region 3. The $\mu^\pm e^\mp$ invariant mass (left) and acoplanarity (right) are displayed for events with zero extra tracks on the $\mu^\pm e^\mp$ vertex and $p_T(\mu^\pm e^\mp) < 30$ GeV. The shaded bands indicate the statistical uncertainty in the background estimation. The signal (open histogram) is shown stacked on top of the backgrounds.

reconstructed vertices to a maximum of 11–20.

The predictions for both the $\gamma\gamma \rightarrow W^+W^-$ signal and the $\gamma\gamma \rightarrow \tau^+\tau^-$ background are rescaled to reflect the contribution of proton dissociation, as derived from the high-mass $\gamma\gamma \rightarrow \mu^+\mu^-$ sample. As described in Section 5, a total uncertainty of 16% is assigned to this factor scale factor F , based on the statistical uncertainty of the high-mass $\gamma\gamma \rightarrow \mu^+\mu^-$ control sample and the difference between the matrix-element and EPA approaches.

As a cross-check we perform several alternative estimates and tests of the nominal background contribution of 0.84 ± 0.15 events. To check the sensitivity to the simulation of the dominant W^+W^- background, we replace the default MADGRAPH sample with a PYTHIA sample normalized to the NLO cross section. The agreement with data in the control region is similar to that of MADGRAPH and results in a total background estimate of 0.71 ± 0.21 (stat.) events in the signal region. Scaling the inclusive W^+W^- background to the central value of the CMS cross section measurement [30], rather than the NLO prediction, would change the total background estimate to 0.88 ± 0.15 events. This change is smaller than the uncertainty on the nominal estimate. The sensitivity to the diffractive component of the W^+W^- background is further tested by varying the cross section between 0% and 200% of the nominal value. This results in a variation of ± 0.03 events in the total background estimate. The contribution from vector boson fusion (VBF), $WW \rightarrow WW$, is estimated using the VBFNLO event generator. No VBF events survive all selections, corresponding to an upper limit of ~ 0.1 events at 95% Confidence Level (CL). The contribution of VBF in the 1–6 tracks control region is estimated to be approximately 0.1 events.

In addition, we take advantage of the lack of correlation between the number of the extra tracks and $p_T(\mu^\pm e^\mp)$ in the main background processes to estimate the background from data using the three control regions defined in Section 6. With uncorrelated variables the relationship between the number of events in each region can be expressed as $N_D/N_A = N_B/N_C$, where N_A , N_B , and N_C represent the backgrounds in the inclusive W^+W^- , $\gamma\gamma \rightarrow \tau^+\tau^-$, and inclusive Drell–Yan $\tau^+\tau^-$ control regions, respectively, and N_D represents the background in the signal region. The background in the signal region is then obtained by solving for N_D , resulting in the expression $N_D = (N_A \times N_B)/N_C$. After subtracting the signal contamination estimated from simulation in each region, the resulting background estimate is 0.77 ± 0.44 (stat.) events, with a

Table 5: Summary of systematic uncertainties.

	Signal uncertainty	Background uncertainty (events)
Trigger and lepton identification	4.2%	0.02
Luminosity	2.2%	0.005
Vertexing efficiency	1.0%	0.005
Exclusivity and pileup dependence	10.0%	0.05
Proton dissociation factor	16.3%	0.02

large statistical uncertainty due to the low statistics in the $\gamma\gamma \rightarrow \tau^+\tau^-$ control region.

We also examine same-sign $\mu^\pm e^\pm$ events in data to check for possible backgrounds not included in the simulation, because the main W^+W^- and $\tau^+\tau^-$ backgrounds considered in the analysis are producing opposite-sign lepton pairs. In the control region which has events containing 1–6 extra tracks we find 8 same-sign events with $p_T(\mu^\pm e^\pm) > 30$ GeV passing all selection criteria and 11 events with $p_T(\mu^\pm e^\pm) < 30$ GeV. No events with fewer than two extra tracks on the $\mu^\pm e^\pm$ vertex are observed in the full data sample.

Although no Drell–Yan $\tau^+\tau^-$ events from the simulation survive all selection criteria, the largest discrepancy between the data sample and the simulated sample is seen in the corresponding control region with 1–6 extra tracks and $p_T(\mu^\pm e^\mp) < 30$ GeV. Therefore we perform a final check by recalculating the $\tau^+\tau^-$ backgrounds using an “embedding” procedure, in which $\mu^+\mu^-$ events are selected in data, and the muons replaced with simulated τ decays to final states containing an electron and a muon [51]. In the Drell–Yan control region the embedded sample predicts 165 ± 4 events compared to 182 observed in the data sample. In the signal region, the total background estimated using the embedded sample is 0.67 ± 0.15 events, which is consistent with the nominal background estimate.

The uncertainty in the background estimate includes the statistical uncertainty of the simulated samples or control samples used to evaluate the backgrounds in the signal region. The uncertainties due to trigger and lepton identification, vertexing efficiency, and the exclusivity selection are also applied to the backgrounds that are taken from simulation. An additional uncertainty of 16% is assigned to the $\gamma\gamma \rightarrow \tau^+\tau^-$ background, reflecting the uncertainty in the normalization of the proton dissociation contribution derived from the $\gamma\gamma \rightarrow \mu^+\mu^-$ control sample.

8 Results

Examining the SM $\gamma\gamma \rightarrow W^+W^-$ signal region, we find two events passing all the selection criteria, compared to the expectation of 2.2 ± 0.4 signal events and 0.84 ± 0.15 background events, including the systematic uncertainties listed in Table 5.

We convert the observed results into a cross section and upper limit for events with zero extra tracks within $|\eta| < 2.4$, using the expression $\sigma = \frac{N}{\epsilon \times A \times \mathcal{L}}$, where N is the number of events observed, and $\epsilon \times A$ is the efficiency times acceptance for a SM-like signal. Correcting for efficiency, acceptance, and backgrounds, the best fit signal cross section times branching fraction is:

$$\sigma(\text{pp} \rightarrow \text{p}^{(*)}W^+W^-\text{p}^{(*)} \rightarrow \text{p}^{(*)}\mu^\pm e^\mp \text{p}^{(*)}) = 2.2_{-2.0}^{+3.3} \text{ fb},$$

with a significance of $\sim 1\sigma$. With statistical uncertainties only, the resulting value of the cross section times branching fraction is $2.2_{-2.0}^{+3.2}$ (stat.) fb.

The observed upper limit is estimated using the Feldman–Cousins method [52] to be 2.6 times

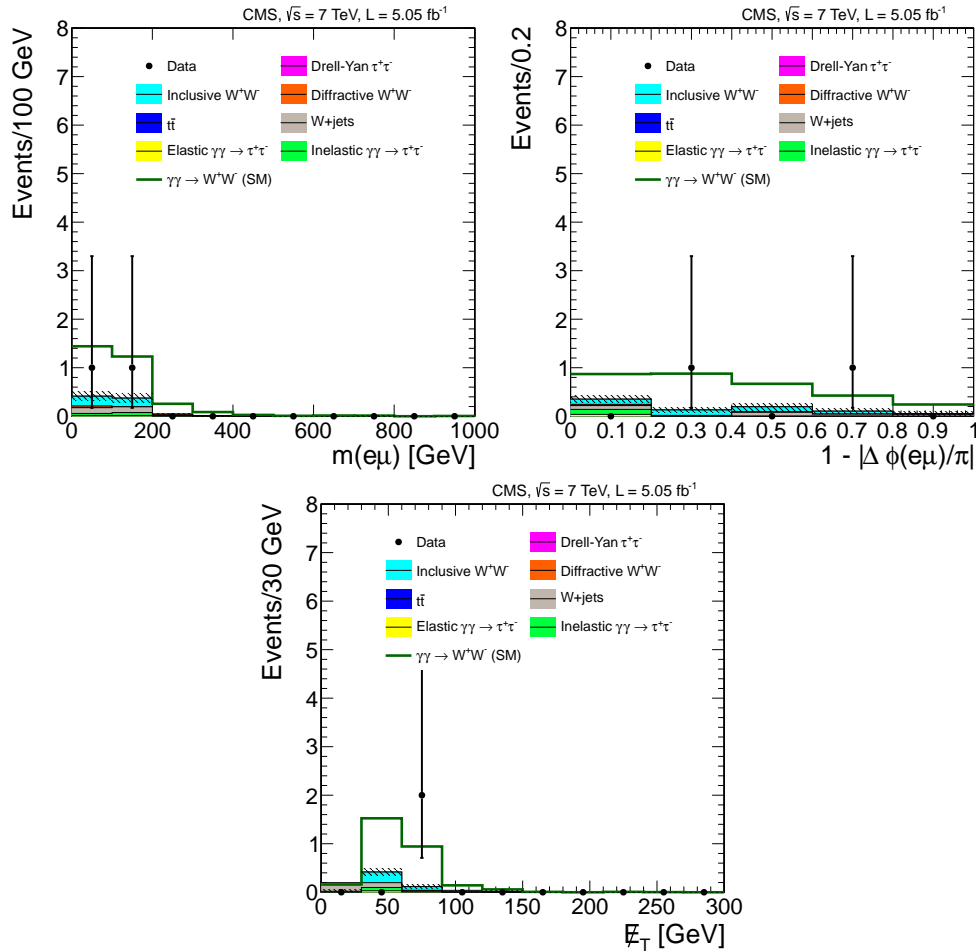


Figure 10: The $\mu^\pm e^\mp$ invariant mass (top left), acoplanarity (top right), and missing transverse energy (bottom) distributions, for events in the signal region with zero extra tracks on the $\mu^\pm e^\mp$ vertex and $p_T(\mu^\pm e^\mp) > 30$ GeV. The backgrounds (solid histograms) are stacked with statistical uncertainties indicated by the shaded region, the signal (open histogram) is stacked on top of the backgrounds.

the expected SM yield at 95% CL. The median expected limit in the absence of signal is $1.5^{+1.0}_{-0.6}$ times the expected SM yield. Converting this to a limit on the cross section we find at 95% CL:

$$\sigma(pp \rightarrow p^{(*)}W^+W^-p^{(*)} \rightarrow p^{(*)}\mu^\pm e^\mp p^{(*)}) < 10.6 \text{ fb.}$$

The SM prediction is 4.0 ± 0.7 fb, including the uncertainty in the contribution of proton dissociation. The dilepton invariant mass, acoplanarity, and missing transverse energy in the two selected events are consistent with the expectation for the sum of backgrounds and SM $\gamma\gamma \rightarrow W^+W^-$ signal (Fig. 10).

The $p_T(\mu^\pm e^\mp)$ distribution for events with zero extra tracks, and the extra tracks multiplicity for events with $p_T(\mu^\pm e^\mp) > 100$ GeV, are shown in Fig. 11. In the anomalous quartic gauge coupling search region $p_T(\mu^\pm e^\mp) > 100$ GeV, zero events are observed in data, which is consistent with the SM expectation of 0.14, dominated by $pp \rightarrow p^{(*)}W^+W^-p^{(*)}$.

We find that the selection efficiency does not vary strongly between the simulated SM and anomalous quartic gauge coupling samples within the detector acceptance (Table 6) and, therefore, set an upper limit on the partial cross section times branching fraction for $\gamma\gamma \rightarrow W^+W^- \rightarrow \mu^\pm e^\mp$ with $p_T(\mu, e) > 20$ GeV, $|\eta(\mu, e)| < 2.4$ (for single leptons), and $p_T(\mu^\pm e^\mp) > 100$ GeV for the pair. We treat the residual SM $pp \rightarrow p^{(*)}W^+W^-p^{(*)}$ signal as a background, resulting in

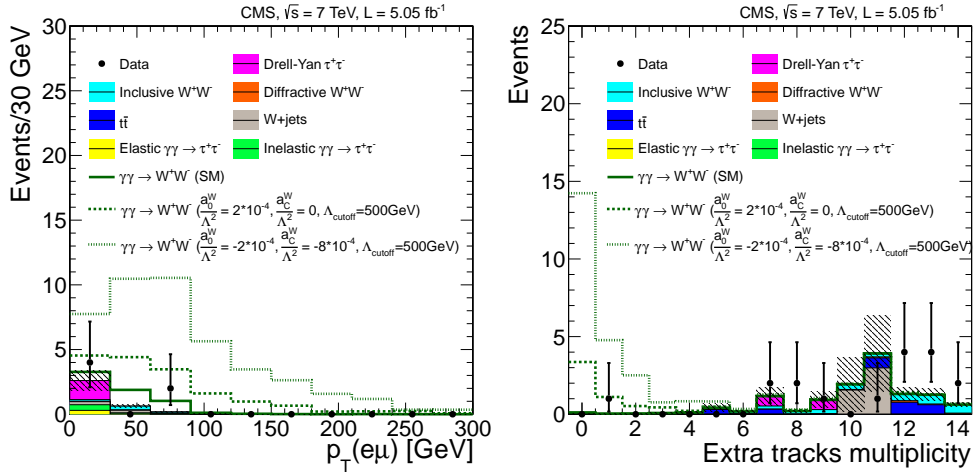


Figure 11: The $p_T(\mu^\pm e^\mp)$ distribution for events with zero extra tracks (left) and multiplicity of extra tracks for events with $p_T(\mu^\pm e^\mp) > 100$ GeV (right). The backgrounds (solid histograms) are stacked with statistical uncertainties indicated by the shaded region, the signal (open histogram) is stacked on top of the backgrounds. The expected signal is shown for the SM $\gamma\gamma \rightarrow W^+W^-$ signal (solid lines) and for two representative values of the anomalous couplings a_0^W/Λ^2 and a_C^W/Λ^2 (dotted and dashed lines).

Table 6: Signal efficiency of all trigger, reconstruction, and analysis selections, relative to the acceptance [$p_T(\mu, e) > 20$ GeV, $|\eta(\mu, e)| < 2.4$, $p_T(\mu^\pm e^\mp) > 100$ GeV] for the SM and for four representative values of the anomalous couplings a_0^W/Λ^2 and a_C^W/Λ^2 , with and without form factors.

a_0^W/Λ^2 [GeV $^{-2}$]	0	2×10^{-4}	-2×10^{-4}	7.5×10^{-6}	0
a_C^W/Λ^2 [GeV $^{-2}$]	0	0	-8×10^{-4}	0	2.5×10^{-5}
Λ [GeV]	–	500	500	No form factor	No form factor
Efficiency	$30.5 \pm 5.0\%$	$29.8 \pm 2.1\%$	$31.3 \pm 1.8\%$	$36.0 \pm 1.7\%$	$36.3 \pm 1.8\%$

a total of 0.14 ± 0.02 expected events, and include an additional systematic uncertainty of 10% based on the maximum relative variation of the efficiency between the SM simulation and the samples generated with two values of the anomalous couplings.

Using the Feldman–Cousins method [52], the 95% CL confidence interval for the Poisson mean for signal events is [0,3.0] if the uncertainty on the background mean is neglected. Inserting the uncertainty on the background into the frequentist interval construction reduces the upper endpoint, as it changes the nature of the problem from a purely discrete observation with typical over-coverage to a continuous problem with exact coverage. To avoid an effect such as this, Cousins and Highland [53] advocated a Bayesian treatment of the nuisance parameter, which in a case such as the present one leaves the upper endpoint essentially unchanged. This results in an upper limit on the partial cross section times branching fraction at 95% CL with the selections $p_T(\mu, e) > 20$ GeV, $|\eta(\mu, e)| < 2.4$, and $p_T(\mu^\pm e^\mp) > 100$ GeV:

$$\sigma(pp \rightarrow p^{(*)}W^+W^-p^{(*)} \rightarrow p^{(*)}\mu^\pm e^\mp p^{(*)}) < 1.9 \text{ fb.}$$

We further investigate the behavior of the limit in different statistical approaches, with and without the systematic uncertainties included as nuisance parameters. The limits derived from a profile likelihood method, a Bayesian method with a flat prior, the Feldman-Cousins method, the Cousins and Highland method, and the CL_5 method [54] range from 1.9 to 3.3 events at 95% CL.

The expected number of events observed as a function of the anomalous quartic gauge coupling

parameters is interpolated from simulated samples and used to construct 95% CL intervals according to the Feldman–Cousins prescription. With a dipole form factor of $\Lambda_{\text{cutoff}} = 500 \text{ GeV}$, the limits obtained on each anomalous quartic gauge coupling parameter with the other fixed to zero are:

$$\begin{aligned} -0.00015 < a_0^W / \Lambda^2 < 0.00015 \text{ GeV}^{-2} & (a_C^W / \Lambda^2 = 0, \Lambda_{\text{cutoff}} = 500 \text{ GeV}), \\ -0.0005 < a_C^W / \Lambda^2 < 0.0005 \text{ GeV}^{-2} & (a_0^W / \Lambda^2 = 0, \Lambda_{\text{cutoff}} = 500 \text{ GeV}). \end{aligned}$$

These limits are approximately 20 times more stringent than the best limits obtained at the Tevatron [5] with a dipole form factor of $\Lambda_{\text{cutoff}} = 500 \text{ GeV}$, and approximately two orders of magnitude more stringent than the best limits obtained at LEP [8, 11, 13].

We perform a similar procedure to derive two dimensional limits on the a_0^W / Λ^2 and a_C^W / Λ^2 parameters. A large number of samples generated with a fast simulation of the CMS detector [55] is used to confirm that the signal efficiency of all trigger, reconstruction, and analysis selections, relative to the acceptance, is flat across the anomalous quartic gauge coupling sample space, and to derive a parameterized dependence of the cross section on the anomalous couplings. The resulting two-dimensional 95% confidence region is shown in Fig. 12, including the form factor with $\Lambda_{\text{cutoff}} = 500 \text{ GeV}$.

We also obtain the corresponding limits without form factors. In this case the cross section is dominated by the region of high energy $\gamma\gamma$ interactions, above the unitarity bound. This leads to one dimensional limits on each of the anomalous couplings, with the other fixed to zero, that are much smaller than in the scenario with form factors:

$$\begin{aligned} -4.0 \times 10^{-6} < a_0^W / \Lambda^2 < 4.0 \times 10^{-6} \text{ GeV}^{-2} & (a_C^W / \Lambda^2 = 0, \text{no form factor}), \\ -1.5 \times 10^{-5} < a_C^W / \Lambda^2 < 1.5 \times 10^{-5} \text{ GeV}^{-2} & (a_0^W / \Lambda^2 = 0, \text{no form factor}). \end{aligned}$$

These limits are approximately two orders of magnitude more restrictive than limits obtained at the Tevatron without form factors [5].

9 Summary

A search for exclusive and quasi-exclusive two-photon production of W^+W^- in the $\mu^\pm e^\mp$ channel, $pp \rightarrow p^{(*)}W^+W^-p^{(*)} \rightarrow p^{(*)}\mu^\pm e^\mp p^{(*)}$, has been performed using 5.05 fb^{-1} of data collected at a center-of-mass energy of 7 TeV by the CMS detector in 2011. The efficiencies and theoretical predictions for the signal have been checked using $\gamma\gamma \rightarrow \mu^+\mu^-$ events, while the backgrounds are constrained from the data using control regions defined by the number of extra tracks and by the p_T of the $\mu^\pm e^\mp$ pair.

In a region sensitive to SM $\gamma\gamma \rightarrow W^+W^-$ production with $p_T(\mu^\pm e^\mp) > 30 \text{ GeV}$, two events are observed, with a background expectation of 0.84 ± 0.15 . The signal expectation is 2.2 ± 0.4 events, with the uncertainty on the theory reflecting the uncertainty on the proton dissociation contribution. The significance of the signal is $\sim 1\sigma$, with a 95% CL upper limit on the SM cross section of 10.6 fb.

In the region with $p_T(\mu^\pm e^\mp) > 100 \text{ GeV}$, where the SM contribution is expected to be small, no events are observed. A limit is set on the partial cross section times branching fraction within the acceptance of $p_T(\mu, e) > 20 \text{ GeV}$, $|\eta(\mu, e)| < 2.4$, $p_T(\mu^\pm e^\mp) > 100 \text{ GeV}$ at 95% CL:

$$\sigma(pp \rightarrow p^{(*)}W^+W^-p^{(*)} \rightarrow p^{(*)}\mu^\pm e^\mp p^{(*)}) < 1.9 \text{ fb.}$$

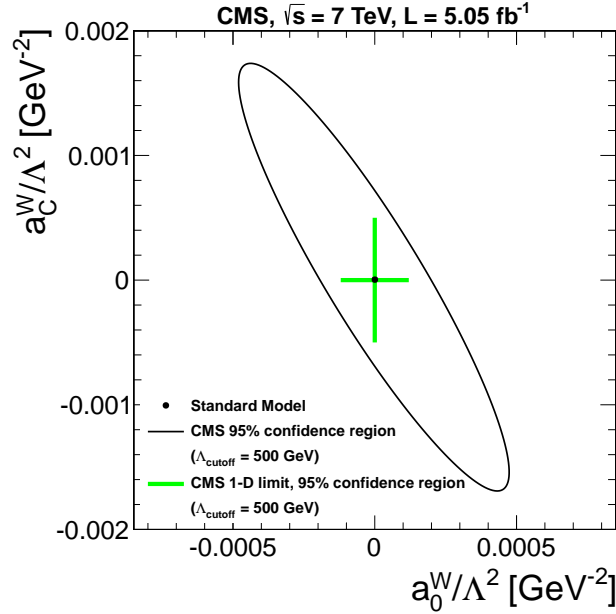


Figure 12: Excluded values of the anomalous coupling parameters a_0^W/Λ^2 and a_C^W/Λ^2 with $\Lambda_{\text{cutoff}} = 500$ GeV. The area outside the solid contour is excluded by this measurement at 95% CL, obtained for $p_T(\mu, e) > 20$ GeV, $|\eta(\mu, e)| < 2.4$, $p_T(\mu^\pm e^\mp) > 100$ GeV. The predicted cross sections are rescaled to include the contribution from proton dissociation.

We use this subsample to set limits on the anomalous quartic gauge coupling parameters, which results in values of the order of $1.5 \times 10^{-4} \text{ GeV}^{-2}$ for a_0^W/Λ^2 and $5 \times 10^{-4} \text{ GeV}^{-2}$ for a_C^W/Λ^2 , assuming a dipole form factor with the energy cutoff scale at $\Lambda_{\text{cutoff}} = 500$ GeV. These limits are approximately 20 times more stringent than the best limits obtained at the Tevatron, and approximately two orders of magnitude more stringent than the best limits obtained at LEP. With no form factors, the limits on the anomalous quartic gauge coupling parameters would be of order 10^{-5} GeV^{-2} and below, driven by high-energy $\gamma\gamma$ interactions beyond the unitarity bound.

Acknowledgments

We congratulate our colleagues in the CERN accelerator departments for the excellent performance of the LHC and thank the technical and administrative staffs at CERN and at other CMS institutes for their contributions to the success of the CMS effort. In addition, we gratefully acknowledge the computing centres and personnel of the Worldwide LHC Computing Grid for delivering so effectively the computing infrastructure essential to our analyses. Finally, we acknowledge the enduring support for the construction and operation of the LHC and the CMS detector provided by the following funding agencies: the Austrian Federal Ministry of Science and Research and the Austrian Science Fund; the Belgian Fonds de la Recherche Scientifique, and Fonds voor Wetenschappelijk Onderzoek; the Brazilian Funding Agencies (CNPq, CAPES, FAPERJ, and FAPESP); the Bulgarian Ministry of Education, Youth and Science; CERN; the Chinese Academy of Sciences, Ministry of Science and Technology, and National Natural Science Foundation of China; the Colombian Funding Agency (COLCIENCIAS); the Croatian Ministry of Science, Education and Sport; the Research Promotion Foundation, Cyprus; the Ministry of Education and Research, Recurrent financing contract SF0690030s09 and European Regional Development Fund, Estonia; the Academy of Finland, Finnish Ministry of Education and Culture, and Helsinki Institute of Physics; the Institut National de Physique Nucléaire et

de Physique des Particules / CNRS, and Commissariat à l'Énergie Atomique et aux Énergies Alternatives / CEA, France; the Bundesministerium für Bildung und Forschung, Deutsche Forschungsgemeinschaft, and Helmholtz-Gemeinschaft Deutscher Forschungszentren, Germany; the General Secretariat for Research and Technology, Greece; the National Scientific Research Foundation, and National Office for Research and Technology, Hungary; the Department of Atomic Energy and the Department of Science and Technology, India; the Institute for Studies in Theoretical Physics and Mathematics, Iran; the Science Foundation, Ireland; the Istituto Nazionale di Fisica Nucleare, Italy; the Korean Ministry of Education, Science and Technology and the World Class University program of NRF, Republic of Korea; the Lithuanian Academy of Sciences; the Mexican Funding Agencies (CINVESTAV, CONACYT, SEP, and UASLP-FAI); the Ministry of Science and Innovation, New Zealand; the Pakistan Atomic Energy Commission; the Ministry of Science and Higher Education and the National Science Centre, Poland; the Fundação para a Ciência e a Tecnologia, Portugal; JINR (Armenia, Belarus, Georgia, Ukraine, Uzbekistan); the Ministry of Education and Science of the Russian Federation, the Federal Agency of Atomic Energy of the Russian Federation, Russian Academy of Sciences, and the Russian Foundation for Basic Research; the Ministry of Science and Technological Development of Serbia; the Secretaría de Estado de Investigación, Desarrollo e Innovación and Programa Consolider-Ingenio 2010, Spain; the Swiss Funding Agencies (ETH Board, ETH Zurich, PSI, SNF, UniZH, Canton Zurich, and SER); the National Science Council, Taipei; the Thailand Center of Excellence in Physics, the Institute for the Promotion of Teaching Science and Technology of Thailand and the National Science and Technology Development Agency of Thailand; the Scientific and Technical Research Council of Turkey, and Turkish Atomic Energy Authority; the Science and Technology Facilities Council, UK; the US Department of Energy, and the US National Science Foundation.

Individuals have received support from the Marie-Curie programme and the European Research Council and EPLANET (European Union); the Leventis Foundation; the A. P. Sloan Foundation; the Alexander von Humboldt Foundation; the Belgian Federal Science Policy Office; the Fonds pour la Formation à la Recherche dans l'Industrie et dans l'Agriculture (FRIA-Belgium); the Agentschap voor Innovatie door Wetenschap en Technologie (IWT-Belgium); the Ministry of Education, Youth and Sports (MEYS) of Czech Republic; the Council of Science and Industrial Research, India; the Compagnia di San Paolo (Torino); the HOMING PLUS programme of Foundation for Polish Science, cofinanced by EU, Regional Development Fund; and the Thalís and Aristeia programmes cofinanced by EU-ESF and the Greek NSRF.

References

- [1] D. d'Enterria, M. Klasen, and K. Piotrkowski, eds., "Photon-LHC-2008. Proceedings of the International Workshop on High-energy Photon Collisions at the LHC". *Nucl. Phys. Proc. Suppl.* **179-180**, (2008). doi:10.1016/S0920-5632(08)00090-X.
- [2] J. de Favereau de Jeneret et al., "High energy photon interactions at the LHC", (2009). arXiv:0908.2020.
- [3] T. Pierzchala and K. Piotrkowski, "Sensitivity to anomalous quartic gauge couplings in photon-photon interactions at the LHC", *Nucl. Phys. Proc. Suppl.* **179-180** (2008) 257, doi:10.1016/j.nuclphysbps.2008.07.032, arXiv:0807.1121.
- [4] E. Chapon, C. Royon, and O. Kepka, "Anomalous quartic $WW\gamma\gamma$, $ZZ\gamma\gamma$, and trilinear $WW\gamma$ couplings in two-photon processes at high luminosity at the LHC", *Phys. Rev. D* **81** (2010) 074003, doi:10.1103/PhysRevD.81.074003, arXiv:0912.5161.

- [5] D0 Collaboration, "Search for anomalous quartic $WW\gamma\gamma$ couplings in dielectron and missing energy final states in $p\bar{p}$ collisions at $\sqrt{s} = 1.96$ TeV", (2013).
arXiv:1305.1258.
- [6] G. Belanger et al., "Bosonic quartic couplings at LEP-2", *Eur. Phys. J. C* **13** (2000) 283,
doi:10.1007/s100520000305, arXiv:hep-ph/9908254.
- [7] ALEPH Collaboration, "Constraints on anomalous QGC's in e^+e^- interactions from 183 GeV to 209 GeV", *Phys. Lett. B* **602** (2004) 31,
doi:10.1016/j.physletb.2004.09.041.
- [8] OPAL Collaboration, "Constraints on anomalous quartic gauge boson couplings from $\nu\bar{\nu}\gamma\gamma$ and $q\bar{q}\gamma\gamma$ events at LEP-2", *Phys. Rev. D* **70** (2004) 032005,
doi:10.1103/PhysRevD.70.032005, arXiv:hep-ex/0402021.
- [9] OPAL Collaboration, "A study of $W^+W^-\gamma$ events at LEP", *Phys. Lett. B* **580** (2004) 17,
doi:10.1016/j.physletb.2003.10.063, arXiv:hep-ex/0309013.
- [10] OPAL Collaboration, "Measurement of the $W^+W^-\gamma$ cross-section and first direct limits on anomalous electroweak quartic gauge couplings", *Phys. Lett. B* **471** (1999) 293,
doi:10.1016/S0370-2693(99)01357-X, arXiv:hep-ex/9910069.
- [11] L3 Collaboration, "The $e^+e^- \rightarrow Z\gamma\gamma \rightarrow q\bar{q}\gamma\gamma$ reaction at LEP and constraints on anomalous quartic gauge boson couplings", *Phys. Lett. B* **540** (2002) 43,
doi:10.1016/S0370-2693(02)02127-5, arXiv:hep-ex/0206050.
- [12] L3 Collaboration, "Study of the $W^+W^-\gamma$ process and limits on anomalous quartic gauge boson couplings at LEP", *Phys. Lett. B* **527** (2002) 29,
doi:10.1016/S0370-2693(02)01167-X, arXiv:hep-ex/0111029.
- [13] DELPHI Collaboration, "Measurement of the $e^+e^- \rightarrow W^+W^-\gamma$ cross-section and limits on anomalous quartic gauge couplings with DELPHI", *Eur. Phys. J. C* **31** (2003) 139,
doi:10.1140/epjc/s2003-01350-x, arXiv:hep-ex/0311004.
- [14] CMS Collaboration, "Exclusive photon-photon production of muon pairs in proton-proton collisions at $\sqrt{s} = 7$ TeV", *JHEP* **01** (2012) 052,
doi:10.1007/JHEP01(2012)052, arXiv:1111.5536.
- [15] CMS Collaboration, "Search for exclusive or semi-exclusive photon pair production and observation of exclusive and semi-exclusive electron pair production in pp collisions at $\sqrt{s} = 7$ TeV", *JHEP* **11** (2012) 080, doi:10.1007/JHEP11(2012)080,
arXiv:1209.1666.
- [16] G. Belanger and F. Boudjema, "Probing quartic couplings of weak bosons through three vectors production at a 500 GeV NLC", *Phys. Lett. B* **288** (1992) 201,
doi:10.1016/0370-2693(92)91978-I.
- [17] CMS Collaboration, "The CMS experiment at the CERN LHC", *JINST* **3** (2008) S08004,
doi:10.1088/1748-0221/3/08/S08004.
- [18] S. L. Glashow, "Partial Symmetries of Weak Interactions", *Nucl. Phys.* **22** (1961) 579,
doi:10.1016/0029-5582(61)90469-2.
- [19] S. Weinberg, "A Model of Leptons", *Phys. Rev. Lett.* **19** (1967) 1264,
doi:10.1103/PhysRevLett.19.1264.

- [20] A. Salam, "Weak and electromagnetic interactions", in *Elementary particle physics: relativistic groups and analyticity*, N. Svartholm, ed., p. 367. Almqvist & Wiskell, 1968. Proceedings of the eighth Nobel symposium.
- [21] D0 Collaboration, "Studies of WW and WZ production and limits on anomalous WW γ and WWZ couplings", (1999). arXiv:hep-ex/9905005.
- [22] D0 Collaboration, "Limits on anomalous trilinear gauge couplings from WW $\rightarrow e^+e^-$, WW $\rightarrow e^\pm\mu^\mp$, and WW $\rightarrow \mu^+\mu^-$ events from $p\bar{p}$ collisions at $\sqrt{s} = 1.96$ TeV", *Phys. Rev. D* **74** (2006) 057101, doi:10.1103/PhysRevD.74.057101, arXiv:hep-ex/0608011. Erratum (corrected title), doi:10.1103/PhysRevD.74.059904.
- [23] A. Pukhov, "CalcHEP 2.3: MSSM, structure functions, event generation, batchs, and generation of matrix elements for other packages", (2004). arXiv:hep-ph/0412191.
- [24] T. Sjöstrand, S. Mrenna, and P. Z. Skands, "PYTHIA 6.4 physics and manual", *JHEP* **05** (2006) 026, doi:10.1088/1126-6708/2006/05/026, arXiv:hep-ph/0603175.
- [25] J. Alwall et al., "MadGraph 5: going beyond", *JHEP* **06** (2011) 128, doi:10.1007/JHEP06(2011)128, arXiv:1106.0522.
- [26] P. Nason, "A new method for combining NLO QCD with shower Monte Carlo algorithms", *JHEP* **11** (2004) 040, doi:10.1088/1126-6708/2004/11/040, arXiv:hep-ph/0409146.
- [27] S. Frixione, P. Nason, and C. Oleari, "Matching NLO QCD computations with parton shower simulations: the POWHEG method", *JHEP* **11** (2007) 070, doi:10.1088/1126-6708/2007/11/070, arXiv:0709.2092.
- [28] S. Alioli, P. Nason, C. Oleari, and E. Re, "A general framework for implementing NLO calculations in shower Monte Carlo programs: the POWHEG BOX", *JHEP* **06** (2010) 043, doi:10.1007/JHEP06(2010)043, arXiv:1002.2581.
- [29] S. Jadach, Z. Was, R. Decker, and J. H. Kuhn, "The tau decay library TAUOLA: Version 2.4", *Comput. Phys. Commun.* **76** (1993) 361, doi:10.1016/0010-4655(93)90061-G.
- [30] CMS Collaboration, "Measurement of the W $^+W^-$ cross section in pp collisions at $\sqrt{s} = 7$ TeV and limits on anomalous WW γ and WWZ couplings", (2013). arXiv:1306.1126. Submitted to Eur. Phys. J. C.
- [31] J. M. Campbell and R. K. Ellis, "MCFM for the Tevatron and the LHC", *Nucl. Phys. Proc. Suppl.* **205-206** (2010) 10, doi:10.1016/j.nuclphysbps.2010.08.011, arXiv:1007.3492.
- [32] CMS Collaboration, "Measurement of W $^+W^-$ production and search for the Higgs boson in pp collisions at $\sqrt{s} = 7$ TeV", *Phys. Lett. B* **699** (2011) 25, doi:10.1016/j.physletb.2011.03.056, arXiv:1102.5429 [hep-ex].
- [33] ATLAS Collaboration, "Measurement of W $^+W^-$ production in pp collisions at $\sqrt{s} = 7$ TeV with the ATLAS detector and limits on anomalous WWZ and WW γ couplings", (2012). arXiv:1210.2979.
- [34] R. Field, "Min-bias and the Underlying Event at the LHC", *Acta Phys. Polon. B* **42** (2011) 2631, doi:10.5506/APhysPolB.42.2631, arXiv:1110.5530.

- [35] P. Bruni and G. Ingelman, "Diffractive hard scattering at ep and $p\bar{p}$ colliders", in *International Europhysics Conference on High-energy Physics, 1993*, p. 595. Editions Frontières, 1994.
- [36] J. A. M. Vermaseren, "Two-photon processes at very high energies", *Nucl. Phys. B* **229** (1983) 347, doi:10.1016/0550-3213(83)90336-X.
- [37] S. P. Baranov, O. Duenger, H. Shooshtari, and J. A. M. Vermaseren, "LPAIR: A generator for lepton pair production", in *Proceedings of Physics at HERA*, volume 3, p. 1478. Hamburg, 1991.
- [38] P. Lebedowicz, R. Pasechnik, and A. Szczurek, "QCD diffractive mechanism of exclusive W^+W^- pair production at high energies", *Nucl. Phys. B* **867** (2013) 61, doi:10.1016/j.nuclphysb.2012.09.014, arXiv:1203.1832.
- [39] K. Arnold et al., "VBFNLO: A parton level Monte Carlo for processes with electroweak Bosons – Manual for Version 2.5.0", (2011). arXiv:1107.4038v1.
- [40] GEANT4 Collaboration, "GEANT4—a simulation toolkit", *Nucl. Instrum. Meth. A* **506** (2003) 250, doi:10.1016/S0168-9002(03)01368-8.
- [41] CMS Collaboration, "Electron reconstruction and identification at $\sqrt{s} = 7$ TeV", CMS Physics Analysis Summary CMS-PAS-EGM-10-004, (2010).
- [42] CMS Collaboration, "Particle-flow event reconstruction in CMS and performance for jets, taus, and MET", CMS Physics Analysis Summary CMS-PAS-PFT-09-001, (2009).
- [43] L. A. Harland-Lang, V. A. Khoze, M. G. Ryskin, and W. J. Stirling, "The phenomenology of central exclusive production at hadron colliders", *Eur. Phys. J. C* **72** (2012) 2110, doi:10.1140/epjc/s10052-012-2110-2, arXiv:1204.4803.
- [44] V. P. Gonçalves and M. V. T. Machado, "Diffractive photoproduction of Z^0 bosons in coherent interactions at CERN LHC", *Eur. Phys. J. C* **56** (2008) 33, doi:10.1140/epjc/s10052-009-1009-z, arXiv:0710.4287.
- [45] L. Motyka and G. Watt, "Exclusive photoproduction at the Tevatron and CERN LHC within the dipole picture", *Phys. Rev. D* **78** (2008) 014023, doi:10.1103/PhysRevD.78.014023, arXiv:0805.2113.
- [46] A. Cisek, W. Schafer, and A. Szczurek, "Production of Z^0 bosons with rapidity gaps: Exclusive photoproduction in γp and pp collisions and inclusive double diffractive Z^0 's", *Phys. Rev. D* **80** (2009) 074013, doi:10.1103/PhysRevD.80.074013, arXiv:0906.1739.
- [47] V. M. Budnev, I. F. Ginzburg, G. V. Meledin, and V. G. Serbo, "The two-photon particle production mechanism. Physical problems. Applications. Equivalent photon approximation", *Phys. Rept.* **15** (1975) 181, doi:10.1016/0370-1573(75)90009-5.
- [48] Particle Data Group, J. Beringer et al., "Review of Particle Physics", *Phys. Rev. D* **86** (2012) 010001, doi:10.1103/PhysRevD.86.010001.
- [49] CMS Collaboration, "Absolute calibration of the luminosity measurement at CMS: Winter 2012 update", CMS Physics Analysis Summary CMS-PAS-SMP-12-008, (2012).

- [50] CMS Collaboration, “Tracking and Primary Vertex Results in First 7 TeV Collisions”, CMS Physics Analysis Summary CMS-PAS-TRK-10-005, (2010).
- [51] CMS Collaboration, “Search for neutral Higgs bosons decaying to τ pairs in pp collisions at $\sqrt{s} = 7$ TeV”, *Phys. Lett. B* **713** (2012) 68, doi:10.1016/j.physletb.2012.05.028, arXiv:1202.4083.
- [52] G. J. Feldman and R. D. Cousins, “A unified approach to the classical statistical analysis of small signals”, *Phys. Rev. D* **57** (1998) 3873, doi:10.1103/PhysRevD.57.3873, arXiv:physics/9711021.
- [53] R. D. Cousins and V. L. Highland, “Incorporating systematic uncertainties into an upper limit”, *Nucl. Instrum. Meth. A* **320** (1992) 331, doi:10.1016/0168-9002(92)90794-5.
- [54] A. L. Read, “Presentation of search results: The CL_s technique”, *J. Phys. G* **28** (2002) 2693, doi:10.1088/0954-3899/28/10/313.
- [55] R. Rahmat, R. Kroeger, and A. Giammanco, “The fast simulation of the CMS experiment”, *J. Phys. Conf. Ser.* **396** (2012) 062016, doi:10.1088/1742-6596/396/6/062016.

A The CMS Collaboration

Yerevan Physics Institute, Yerevan, Armenia

S. Chatrchyan, V. Khachatryan, A.M. Sirunyan, A. Tumasyan

Institut für Hochenergiephysik der OeAW, Wien, Austria

W. Adam, T. Bergauer, M. Dragicevic, J. Erö, C. Fabjan¹, M. Friedl, R. Frühwirth¹, V.M. Ghete, N. Hörmann, J. Hrubec, M. Jeitler¹, W. Kiesenhofer, V. Knünz, M. Krammer¹, I. Krätschmer, D. Liko, I. Mikulec, D. Rabady², B. Rahbaran, C. Rohringer, H. Rohringer, R. Schöfbeck, J. Strauss, A. Taurok, W. Treberer-Treberspurg, W. Waltenberger, C.-E. Wulz¹

National Centre for Particle and High Energy Physics, Minsk, Belarus

V. Mossolov, N. Shumeiko, J. Suarez Gonzalez

Universiteit Antwerpen, Antwerpen, Belgium

S. Alderweireldt, M. Bansal, S. Bansal, T. Cornelis, E.A. De Wolf, X. Janssen, A. Knutsson, S. Luyckx, L. Mucibello, S. Ochesanu, B. Roland, R. Rougny, H. Van Haeuvermaet, P. Van Mechelen, N. Van Remortel, A. Van Spilbeeck

Vrije Universiteit Brussel, Brussel, Belgium

F. Blekman, S. Blyweert, J. D'Hondt, A. Kalogeropoulos, J. Keaveney, M. Maes, A. Olbrechts, S. Tavernier, W. Van Doninck, P. Van Mulders, G.P. Van Onsem, I. Villella

Université Libre de Bruxelles, Bruxelles, Belgium

B. Clerbaux, G. De Lentdecker, L. Favart, A.P.R. Gay, T. Hreus, A. Léonard, P.E. Marage, A. Mohammadi, L. Perniè, T. Reis, T. Seva, L. Thomas, C. Vander Velde, P. Vanlaer, J. Wang

Ghent University, Ghent, Belgium

V. Adler, K. Beernaert, L. Benucci, A. Cimmino, S. Costantini, S. Dildick, G. Garcia, B. Klein, J. Lellouch, A. Marinov, J. Mccartin, A.A. Ocampo Rios, D. Ryckbosch, M. Sigamani, N. Strobbe, F. Thyssen, M. Tytgat, S. Walsh, E. Yazgan, N. Zaganidis

Université Catholique de Louvain, Louvain-la-Neuve, Belgium

S. Basegmez, C. Beluffi³, G. Bruno, R. Castello, A. Caudron, L. Ceard, G.G. Da Silva, C. Delaere, T. du Pree, D. Favart, L. Forthomme, A. Giammanco⁴, J. Hollar, P. Jez, V. Lemaître, J. Liao, O. Militaru, C. Nuttens, D. Pagano, A. Pin, K. Piotrkowski, A. Popov⁵, M. Selvaggi, J.M. Vizan Garcia

Université de Mons, Mons, Belgium

N. Belyi, T. Caebergs, E. Daubie, G.H. Hammad

Centro Brasileiro de Pesquisas Fisicas, Rio de Janeiro, Brazil

G.A. Alves, M. Correa Martins Junior, T. Martins, M.E. Pol, M.H.G. Souza

Universidade do Estado do Rio de Janeiro, Rio de Janeiro, Brazil

W.L. Aldá Júnior, W. Carvalho, J. Chinellato⁶, A. Custódio, E.M. Da Costa, D. De Jesus Damiao, C. De Oliveira Martins, S. Fonseca De Souza, H. Malbouisson, M. Malek, D. Matos Figueiredo, L. Mundim, H. Nogima, W.L. Prado Da Silva, A. Santoro, L. Soares Jorge, A. Sznajder, E.J. Tonelli Manganote⁶, A. Vilela Pereira

Universidade Estadual Paulista ^a, Universidade Federal do ABC ^b, São Paulo, Brazil

T.S. Anjos^b, C.A. Bernardes^b, F.A. Dias^{a,7}, T.R. Fernandez Perez Tomei^a, E.M. Gregores^b, C. Lagana^a, F. Marinho^a, P.G. Mercadante^b, S.F. Novaes^a, Sandra S. Padula^a

Institute for Nuclear Research and Nuclear Energy, Sofia, Bulgaria

V. Genchev², P. Iaydjiev², S. Piperov, M. Rodozov, G. Sultanov, M. Vutova

University of Sofia, Sofia, Bulgaria

A. Dimitrov, R. Hadjiiska, V. Kozhuharov, L. Litov, B. Pavlov, P. Petkov

Institute of High Energy Physics, Beijing, China

J.G. Bian, G.M. Chen, H.S. Chen, C.H. Jiang, D. Liang, S. Liang, X. Meng, J. Tao, J. Wang, X. Wang, Z. Wang, H. Xiao, M. Xu

State Key Laboratory of Nuclear Physics and Technology, Peking University, Beijing, China

C. Asawatrangkuldee, Y. Ban, Y. Guo, Q. Li, W. Li, S. Liu, Y. Mao, S.J. Qian, D. Wang, L. Zhang, W. Zou

Universidad de Los Andes, Bogota, Colombia

C. Avila, C.A. Carrillo Montoya, J.P. Gomez, B. Gomez Moreno, J.C. Sanabria

Technical University of Split, Split, Croatia

N. Godinovic, D. Lelas, R. Plestina⁸, D. Polic, I. Puljak

University of Split, Split, Croatia

Z. Antunovic, M. Kovac

Institute Rudjer Boskovic, Zagreb, Croatia

V. Brigljevic, S. Duric, K. Kadija, J. Luetic, D. Mekterovic, S. Morovic, L. Tikvica

University of Cyprus, Nicosia, Cyprus

A. Attikis, G. Mavromanolakis, J. Mousa, C. Nicolaou, F. Ptochos, P.A. Razis

Charles University, Prague, Czech Republic

M. Finger, M. Finger Jr.

Academy of Scientific Research and Technology of the Arab Republic of Egypt, Egyptian Network of High Energy Physics, Cairo, Egypt

Y. Assran⁹, A. Ellithi Kamel¹⁰, M.A. Mahmoud¹¹, A. Mahrous¹², A. Radi^{13,14}

National Institute of Chemical Physics and Biophysics, Tallinn, Estonia

M. Kadastik, M. Müntel, M. Murumaa, M. Raidal, L. Rebane, A. Tiko

Department of Physics, University of Helsinki, Helsinki, Finland

P. Eerola, G. Fedi, M. Voutilainen

Helsinki Institute of Physics, Helsinki, Finland

J. Härkönen, V. Karimäki, R. Kinnunen, M.J. Kortelainen, T. Lampén, K. Lassila-Perini, S. Lehti, T. Lindén, P. Luukka, T. Mäenpää, T. Peltola, E. Tuominen, J. Tuominiemi, E. Tuovinen, L. Wendland

Lappeenranta University of Technology, Lappeenranta, Finland

A. Korpela, T. Tuuva

DSM/IRFU, CEA/Saclay, Gif-sur-Yvette, France

M. Besancon, S. Choudhury, F. Couderc, M. Dejardin, D. Denegri, B. Fabbro, J.L. Faure, F. Ferri, S. Ganjour, A. Givernaud, P. Gras, G. Hamel de Monchenault, P. Jarry, E. Locci, J. Malcles, L. Millischer, A. Nayak, J. Rander, A. Rosowsky, M. Titov

Laboratoire Leprince-Ringuet, Ecole Polytechnique, IN2P3-CNRS, Palaiseau, France

S. Baffioni, F. Beaudette, L. Benhabib, L. Bianchini, M. Bluj¹⁵, P. Busson, C. Charlot, N. Daci, T. Dahms, M. Dalchenko, L. Dobrzynski, A. Florent, R. Granier de Cassagnac, M. Haguenaer, P. Miné, C. Mironov, I.N. Naranjo, M. Nguyen, C. Ochando, P. Paganini, D. Sabes, R. Salerno, Y. Sirois, C. Veelken, A. Zabi

Institut Pluridisciplinaire Hubert Curien, Université de Strasbourg, Université de Haute Alsace Mulhouse, CNRS/IN2P3, Strasbourg, France

J.-L. Agram¹⁶, J. Andrea, D. Bloch, D. Bodin, J.-M. Brom, E.C. Chabert, C. Collard, E. Conte¹⁶, F. Drouhin¹⁶, J.-C. Fontaine¹⁶, D. Gelé, U. Goerlach, C. Goetzmann, P. Juillot, A.-C. Le Bihan, P. Van Hove

Centre de Calcul de l'Institut National de Physique Nucleaire et de Physique des Particules, CNRS/IN2P3, Villeurbanne, France

S. Gadrat

Université de Lyon, Université Claude Bernard Lyon 1, CNRS-IN2P3, Institut de Physique Nucléaire de Lyon, Villeurbanne, France

S. Beauceron, N. Beaupere, G. Boudoul, S. Brochet, J. Chasserat, R. Chierici, D. Contardo, P. Depasse, H. El Mamouni, J. Fay, S. Gascon, M. Gouzevitch, B. Ille, T. Kurca, M. Lethuillier, L. Mirabito, S. Perries, L. Sgandurra, V. Sordini, Y. Tschudi, M. Vander Donckt, P. Verdier, S. Viret

Institute of High Energy Physics and Informatization, Tbilisi State University, Tbilisi, Georgia

Z. Tsamalaidze¹⁷

RWTH Aachen University, I. Physikalisches Institut, Aachen, Germany

C. Autermann, S. Beranek, B. Calpas, M. Edelhoff, L. Feld, N. Heracleous, O. Hindrichs, K. Klein, J. Merz, A. Ostapchuk, A. Perieanu, F. Raupach, J. Sammet, S. Schael, D. Sprenger, H. Weber, B. Wittmer, V. Zhukov⁵

RWTH Aachen University, III. Physikalisches Institut A, Aachen, Germany

M. Ata, J. Caudron, E. Dietz-Laursonn, D. Duchardt, M. Erdmann, R. Fischer, A. Güth, T. Hebbeker, C. Heidemann, K. Hoepfner, D. Klingebiel, P. Kreuzer, M. Merschmeyer, A. Meyer, M. Olschewski, K. Padeken, P. Papacz, H. Pieta, H. Reithler, S.A. Schmitz, L. Sonnenschein, J. Steggemann, D. Teyssier, S. Thüer, M. Weber

RWTH Aachen University, III. Physikalisches Institut B, Aachen, Germany

V. Cherepanov, Y. Erdogan, G. Flügge, H. Geenen, M. Geisler, W. Haj Ahmad, F. Hoehle, B. Kargoll, T. Kress, Y. Kuessel, J. Lingemann², A. Nowack, I.M. Nugent, L. Perchalla, O. Pooth, A. Stahl

Deutsches Elektronen-Synchrotron, Hamburg, Germany

M. Aldaya Martin, I. Asin, N. Bartosik, J. Behr, W. Behrenhoff, U. Behrens, M. Bergholz¹⁸, A. Bethani, K. Borras, A. Burgmeier, A. Cakir, L. Calligaris, A. Campbell, F. Costanza, C. Diez Pardos, S. Dooling, T. Dorland, G. Eckerlin, D. Eckstein, G. Flucke, A. Geiser, I. Glushkov, P. Gunnellini, S. Habib, J. Hauk, G. Hellwig, H. Jung, M. Kasemann, P. Katsas, C. Kleinwort, H. Kluge, M. Krämer, D. Krücker, E. Kuznetsova, W. Lange, J. Leonard, K. Lipka, W. Lohmann¹⁸, B. Lutz, R. Mankel, I. Marfin, I.-A. Melzer-Pellmann, A.B. Meyer, J. Mnich, A. Mussgiller, S. Naumann-Emme, O. Novgorodova, F. Nowak, J. Olzem, H. Perrey, A. Petrukhin, D. Pitzl, R. Placakyte, A. Raspereza, P.M. Ribeiro Cipriano, C. Riedl, E. Ron, M.Ö. Sahin, J. Salfeld-Nebgen, R. Schmidt¹⁸, T. Schoerner-Sadenius, N. Sen, M. Stein, R. Walsh, C. Wissing

University of Hamburg, Hamburg, Germany

V. Blobel, H. Enderle, J. Erfle, U. Gebbert, M. Görner, M. Gosselink, J. Haller, K. Heine, R.S. Höing, G. Kaussen, H. Kirschenmann, R. Klanner, R. Kogler, J. Lange, I. Marchesini, T. Peiffer, N. Pietsch, D. Rathjens, C. Sander, H. Schettler, P. Schleper, E. Schlieckau, A. Schmidt,

M. Schröder, T. Schum, M. Seidel, J. Sibille¹⁹, V. Sola, H. Stadie, G. Steinbrück, J. Thomsen, D. Troendle, L. Vanelderen

Institut für Experimentelle Kernphysik, Karlsruhe, Germany

C. Barth, C. Baus, J. Berger, C. Böser, T. Chwalek, W. De Boer, A. Descroix, A. Dierlamm, M. Feindt, M. Guthoff², C. Hackstein, F. Hartmann², T. Hauth², M. Heinrich, H. Held, K.H. Hoffmann, U. Husemann, I. Katkov⁵, J.R. Komaragiri, A. Kornmayer², P. Lobelle Pardo, D. Martschei, S. Mueller, Th. Müller, M. Niegel, A. Nürnberg, O. Oberst, J. Ott, G. Quast, K. Rabbertz, F. Ratnikov, S. Röcker, F.-P. Schilling, G. Schott, H.J. Simonis, F.M. Stober, R. Ulrich, J. Wagner-Kuhr, S. Wayand, T. Weiler, M. Zeise

Institute of Nuclear and Particle Physics (INPP), NCSR Demokritos, Aghia Paraskevi, Greece

G. Anagnostou, G. Daskalakis, T. Gerasis, S. Kesisoglou, A. Kyriakis, D. Loukas, A. Markou, C. Markou, E. Ntomari

University of Athens, Athens, Greece

L. Gouskos, T.J. Mertzimekis, A. Panagiotou, N. Saoulidou, E. Stiliaris

University of Ioánnina, Ioánnina, Greece

X. Aslanoglou, I. Evangelou, G. Flouris, C. Foudas, P. Kokkas, N. Manthos, I. Papadopoulos, E. Paradas

KFKI Research Institute for Particle and Nuclear Physics, Budapest, Hungary

G. Bencze, C. Hajdu, P. Hidas, D. Horvath²⁰, B. Radics, F. Sikler, V. Veszpremi, G. Vesztergombi²¹, A.J. Zsigmond

Institute of Nuclear Research ATOMKI, Debrecen, Hungary

N. Beni, S. Czellar, J. Molnar, J. Palinkas, Z. Szillasi

University of Debrecen, Debrecen, Hungary

J. Karacsi, P. Raics, Z.L. Trocsanyi, B. Ujvari

Panjab University, Chandigarh, India

S.B. Beri, V. Bhatnagar, N. Dhingra, R. Gupta, M. Kaur, M.Z. Mehta, M. Mittal, N. Nishu, L.K. Saini, A. Sharma, J.B. Singh

University of Delhi, Delhi, India

Ashok Kumar, Arun Kumar, S. Ahuja, A. Bhardwaj, B.C. Choudhary, S. Malhotra, M. Naimuddin, K. Ranjan, P. Saxena, V. Sharma, R.K. Shivpuri

Saha Institute of Nuclear Physics, Kolkata, India

S. Banerjee, S. Bhattacharya, K. Chatterjee, S. Dutta, B. Gomber, Sa. Jain, Sh. Jain, R. Khurana, A. Modak, S. Mukherjee, D. Roy, S. Sarkar, M. Sharan

Bhabha Atomic Research Centre, Mumbai, India

A. Abdulsalam, D. Dutta, S. Kailas, V. Kumar, A.K. Mohanty², L.M. Pant, P. Shukla, A. Topkar

Tata Institute of Fundamental Research - EHEP, Mumbai, India

T. Aziz, R.M. Chatterjee, S. Ganguly, S. Ghosh, M. Guchait²², A. Gurtu²³, G. Kole, S. Kumar, M. Maity²⁴, G. Majumder, K. Mazumdar, G.B. Mohanty, B. Parida, K. Sudhakar, N. Wickramage²⁵

Tata Institute of Fundamental Research - HECR, Mumbai, India

S. Banerjee, S. Dugad

Institute for Research in Fundamental Sciences (IPM), Tehran, Iran

H. Arfaei²⁶, H. Bakhshiansohi, S.M. Etesami²⁷, A. Fahim²⁶, H. Hesari, A. Jafari, M. Khakzad, M. Mohammadi Najafabadi, S. Paktinat Mehdiabadi, B. Safarzadeh²⁸, M. Zeinali

University College Dublin, Dublin, Ireland

M. Grunewald

INFN Sezione di Bari ^a, Università di Bari ^b, Politecnico di Bari ^c, Bari, Italy

M. Abbrescia^{a,b}, L. Barbone^{a,b}, C. Calabria^{a,b}, S.S. Chhibra^{a,b}, A. Colaleo^a, D. Creanza^{a,c}, N. De Filippis^{a,c,2}, M. De Palma^{a,b}, L. Fiore^a, G. Iaselli^{a,c}, G. Maggi^{a,c}, M. Maggi^a, B. Marangelli^{a,b}, S. My^{a,c}, S. Nuzzo^{a,b}, N. Pacifico^a, A. Pompili^{a,b}, G. Pugliese^{a,c}, G. Selvaggi^{a,b}, L. Silvestris^a, G. Singh^{a,b}, R. Venditti^{a,b}, P. Verwilligen^a, G. Zito^a

INFN Sezione di Bologna ^a, Università di Bologna ^b, Bologna, Italy

G. Abbiendi^a, A.C. Benvenuti^a, D. Bonacorsi^{a,b}, S. Braibant-Giacomelli^{a,b}, L. Brigliadori^{a,b}, R. Campanini^{a,b}, P. Capiluppi^{a,b}, A. Castro^{a,b}, F.R. Cavallo^a, M. Cuffiani^{a,b}, G.M. Dallavalle^a, F. Fabbri^a, A. Fanfani^{a,b}, D. Fasanella^{a,b}, P. Giacomelli^a, C. Grandi^a, L. Guiducci^{a,b}, S. Marcellini^a, G. Masetti^{a,2}, M. Meneghelli^{a,b}, A. Montanari^a, F.L. Navarria^{a,b}, F. Odorici^a, A. Perrotta^a, F. Primavera^{a,b}, A.M. Rossi^{a,b}, T. Rovelli^{a,b}, G.P. Siroli^{a,b}, N. Tosi^{a,b}, R. Travaglini^{a,b}

INFN Sezione di Catania ^a, Università di Catania ^b, Catania, Italy

S. Albergo^{a,b}, M. Chiorboli^{a,b}, S. Costa^{a,b}, F. Giordano^{a,2}, R. Potenza^{a,b}, A. Tricomi^{a,b}, C. Tuve^{a,b}

INFN Sezione di Firenze ^a, Università di Firenze ^b, Firenze, Italy

G. Barbagli^a, V. Ciulli^{a,b}, C. Civinini^a, R. D'Alessandro^{a,b}, E. Focardi^{a,b}, S. Frosali^{a,b}, E. Gallo^a, S. Gonzi^{a,b}, V. Gori^{a,b}, P. Lenzi^{a,b}, M. Meschini^a, S. Paoletti^a, G. Sguazzoni^a, A. Tropiano^{a,b}

INFN Laboratori Nazionali di Frascati, Frascati, Italy

L. Benussi, S. Bianco, F. Fabbri, D. Piccolo

INFN Sezione di Genova ^a, Università di Genova ^b, Genova, Italy

P. Fabbricatore^a, R. Musenich^a, S. Tosi^{a,b}

INFN Sezione di Milano-Bicocca ^a, Università di Milano-Bicocca ^b, Milano, Italy

A. Benaglia^a, F. De Guio^{a,b}, L. Di Matteo^{a,b}, S. Fiorendi^{a,b}, S. Gennai^a, A. Ghezzi^{a,b}, P. Govoni, M.T. Lucchini², S. Malvezzi^a, R.A. Manzoni^{a,b,2}, A. Martelli^{a,b,2}, A. Massironi^{a,b}, D. Menasce^a, L. Moroni^a, M. Paganoni^{a,b}, D. Pedrini^a, S. Ragazzi^{a,b}, N. Redaelli^a, T. Tabarelli de Fatis^{a,b}

INFN Sezione di Napoli ^a, Università di Napoli 'Federico II' ^b, Università della Basilicata (Potenza) ^c, Università G. Marconi (Roma) ^d, Napoli, Italy

S. Buontempo^a, N. Cavallo^{a,c}, A. De Cosa^{a,b}, F. Fabozzi^{a,c}, A.O.M. Iorio^{a,b}, L. Lista^a, S. Meola^{a,d,2}, M. Merola^a, P. Paolucci^{a,2}

INFN Sezione di Padova ^a, Università di Padova ^b, Università di Trento (Trento) ^c, Padova, Italy

P. Azzi^a, N. Bacchetta^a, M. Biasotto^{a,29}, D. Bisello^{a,b}, A. Branca^{a,b}, R. Carlin^{a,b}, P. Checchia^a, T. Dorigo^a, S. Fantinel^a, F. Fanzago^a, M. Galanti^{a,b,2}, F. Gasparini^{a,b}, U. Gasparini^{a,b}, P. Giubileo^{a,b}, A. Gozzelino^a, K. Kanishchev^{a,c}, S. Lacaprara^a, I. Lazzizzera^{a,c}, M. Margoni^{a,b}, A.T. Meneguzzo^{a,b}, J. Pazzini^{a,b}, N. Pozzobon^{a,b}, P. Ronchese^{a,b}, F. Simonetto^{a,b}, E. Torassa^a, M. Tosi^{a,b}, A. Triossi^a, S. Vanini^{a,b}, P. Zotto^{a,b}, G. Zumerle^{a,b}

INFN Sezione di Pavia ^a, Università di Pavia ^b, Pavia, Italy

M. Gabusi^{a,b}, S.P. Ratti^{a,b}, C. Riccardi^{a,b}, P. Vitulo^{a,b}

INFN Sezione di Perugia ^a, Università di Perugia ^b, Perugia, Italy

M. Biasini^{a,b}, G.M. Bilei^a, L. Fanò^{a,b}, P. Lariccia^{a,b}, G. Mantovani^{a,b}, M. Menichelli^a, A. Nappi^{a,b,†}, F. Romeo^{a,b}, A. Saha^a, A. Santocchia^{a,b}, A. Spiezia^{a,b}

INFN Sezione di Pisa ^a, Università di Pisa ^b, Scuola Normale Superiore di Pisa ^c, Pisa, Italy

K. Androsov^{a,30}, P. Azzurri^a, G. Bagliesi^a, T. Boccali^a, G. Broccolo^{a,c}, R. Castaldi^a, R.T. D'Agnolo^{a,c,2}, R. Dell'Orso^a, F. Fiori^{a,c}, L. Foà^{a,c}, A. Giassi^a, A. Kraan^a, F. Ligabue^{a,c}, T. Lomtadze^a, L. Martini^{a,30}, A. Messineo^{a,b}, F. Palla^a, A. Rizzi^{a,b}, A.T. Serban^a, P. Spagnolo^a, P. Squillacioti^a, R. Tenchini^a, G. Tonelli^{a,b}, A. Venturi^a, P.G. Verdini^a, C. Vernieri^{a,c}

INFN Sezione di Roma ^a, Università di Roma ^b, Roma, Italy

L. Barone^{a,b}, F. Cavallari^a, D. Del Re^{a,b}, M. Diemoz^a, M. Grassi^{a,b,2}, E. Longo^{a,b}, F. Margaroli^{a,b}, P. Meridiani^a, F. Micheli^{a,b}, S. Nourbakhsh^{a,b}, G. Organtini^{a,b}, R. Paramatti^a, S. Rahatlou^{a,b}, L. Soffi^{a,b}

INFN Sezione di Torino ^a, Università di Torino ^b, Università del Piemonte Orientale (Novara) ^c, Torino, Italy

N. Amapane^{a,b}, R. Arcidiacono^{a,c}, S. Argiro^{a,b}, M. Arneodo^{a,c}, C. Biino^a, N. Cartiglia^a, S. Casasso^{a,b}, M. Costa^{a,b}, P. De Remigis^a, N. Demaria^a, C. Mariotti^a, S. Maselli^a, E. Migliore^{a,b}, V. Monaco^{a,b}, M. Musich^a, M.M. Obertino^{a,c}, N. Pastrone^a, M. Pelliccioni^{a,2}, A. Potenza^{a,b}, A. Romero^{a,b}, M. Ruspa^{a,c}, R. Sacchi^{a,b}, A. Solano^{a,b}, A. Staiano^a, U. Tamponi^a

INFN Sezione di Trieste ^a, Università di Trieste ^b, Trieste, Italy

S. Belforte^a, V. Candelise^{a,b}, M. Casarsa^a, F. Cossutti^{a,2}, G. Della Ricca^{a,b}, B. Gobbo^a, C. La Licata^{a,b}, M. Marone^{a,b}, D. Montanino^{a,b}, A. Penzo^a, A. Schizzi^{a,b}, A. Zanetti^a

Kangwon National University, Chunchon, Korea

T.Y. Kim, S.K. Nam

Kyungpook National University, Daegu, Korea

S. Chang, D.H. Kim, G.N. Kim, J.E. Kim, D.J. Kong, Y.D. Oh, H. Park, D.C. Son

Chonnam National University, Institute for Universe and Elementary Particles, Kwangju, Korea

J.Y. Kim, Zero J. Kim, S. Song

Korea University, Seoul, Korea

S. Choi, D. Gyun, B. Hong, M. Jo, H. Kim, T.J. Kim, K.S. Lee, S.K. Park, Y. Roh

University of Seoul, Seoul, Korea

M. Choi, J.H. Kim, C. Park, I.C. Park, S. Park, G. Ryu

Sungkyunkwan University, Suwon, Korea

Y. Choi, Y.K. Choi, J. Goh, M.S. Kim, E. Kwon, B. Lee, J. Lee, S. Lee, H. Seo, I. Yu

Vilnius University, Vilnius, Lithuania

I. Grigelionis, A. Juodagalvis

Centro de Investigacion y de Estudios Avanzados del IPN, Mexico City, Mexico

H. Castilla-Valdez, E. De La Cruz-Burelo, I. Heredia-de La Cruz³¹, R. Lopez-Fernandez, J. Martínez-Ortega, A. Sanchez-Hernandez, L.M. Villasenor-Cendejas

Universidad Iberoamericana, Mexico City, Mexico

S. Carrillo Moreno, F. Vazquez Valencia

Benemerita Universidad Autonoma de Puebla, Puebla, Mexico

H.A. Salazar Ibarguen

Universidad Autónoma de San Luis Potosí, San Luis Potosí, Mexico

E. Casimiro Linares, A. Morelos Pineda, M.A. Reyes-Santos

University of Auckland, Auckland, New Zealand

D. Krofcheck

University of Canterbury, Christchurch, New Zealand

A.J. Bell, P.H. Butler, R. Doesburg, S. Reucroft, H. Silverwood

National Centre for Physics, Quaid-I-Azam University, Islamabad, Pakistan

M. Ahmad, M.I. Asghar, J. Butt, H.R. Hoorani, S. Khalid, W.A. Khan, T. Khurshid, S. Qazi, M.A. Shah, M. Shoaib

National Centre for Nuclear Research, Swierk, Poland

H. Bialkowska, B. Boimska, T. Frueboes, M. Górski, M. Kazana, K. Nawrocki, K. Romanowska-Rybinska, M. Szleper, G. Wrochna, P. Zalewski

Institute of Experimental Physics, Faculty of Physics, University of Warsaw, Warsaw, Poland

G. Brona, K. Bunkowski, M. Cwiok, W. Dominik, K. Doroba, A. Kalinowski, M. Konecki, J. Krolikowski, M. Misiura, W. Wolszczak

Laboratório de Instrumentação e Física Experimental de Partículas, Lisboa, PortugalN. Almeida, P. Bargassa, A. David, P. Faccioli, P.G. Ferreira Parracho, M. Gallinaro, J. Rodrigues Antunes, J. Seixas², J. Varela, P. Vischia**Joint Institute for Nuclear Research, Dubna, Russia**

S. Afanasiev, P. Bunin, M. Gavrilenko, I. Golutvin, A. Kamenev, V. Karjavin, V. Konoplyanikov, G. Kozlov, A. Lanev, A. Malakhov, V. Matveev, P. Moisenz, V. Palichik, V. Perelygin, S. Shmatov, N. Skatchkov, V. Smirnov, A. Zarubin

Petersburg Nuclear Physics Institute, Gatchina (St. Petersburg), Russia

S. Evstyukhin, V. Golovtsov, Y. Ivanov, V. Kim, P. Levchenko, V. Murzin, V. Oreshkin, I. Smirnov, V. Sulimov, L. Uvarov, S. Vavilov, A. Vorobyev, An. Vorobyev

Institute for Nuclear Research, Moscow, Russia

Yu. Andreev, A. Dermenev, S. Gninenko, N. Golubev, M. Kirsanov, N. Krasnikov, A. Pashenkov, D. Tlisov, A. Toropin

Institute for Theoretical and Experimental Physics, Moscow, Russia

V. Epshteyn, M. Erofeeva, V. Gavrilov, N. Lychkovskaya, V. Popov, G. Safronov, S. Semenov, A. Spiridonov, V. Stolin, E. Vlasov, A. Zhokin

P.N. Lebedev Physical Institute, Moscow, Russia

V. Andreev, M. Azarkin, I. Dremin, M. Kirakosyan, A. Leonidov, G. Mesyats, S.V. Rusakov, A. Vinogradov

Skobeltsyn Institute of Nuclear Physics, Lomonosov Moscow State University, Moscow, RussiaA. Belyaev, E. Boos, M. Dubinin⁷, A. Ershov, L. Khein, V. Klyukhin, O. Kodolova, I. Lokhtin, A. Markina, S. Obraztsov, S. Petrushanko, A. Proskuryakov, V. Savrin, A. Snigirev

State Research Center of Russian Federation, Institute for High Energy Physics, Protvino, Russia

I. Azhgirey, I. Bayshev, S. Bitioukov, V. Kachanov, A. Kalinin, D. Konstantinov, V. Krychkin, V. Petrov, R. Ryutin, A. Sobol, L. Tourtchanovitch, S. Troshin, N. Tyurin, A. Uzunian, A. Volkov

University of Belgrade, Faculty of Physics and Vinca Institute of Nuclear Sciences, Belgrade, Serbia

P. Adzic³², M. Ekmedzic, D. Krpic³², J. Milosevic

Centro de Investigaciones Energéticas Medioambientales y Tecnológicas (CIEMAT), Madrid, Spain

M. Aguilar-Benitez, J. Alcaraz Maestre, C. Battilana, E. Calvo, M. Cerrada, M. Chamizo Llatas², N. Colino, B. De La Cruz, A. Delgado Peris, D. Domínguez Vázquez, C. Fernandez Bedoya, J.P. Fernández Ramos, A. Ferrando, J. Flix, M.C. Fouz, P. Garcia-Abia, O. Gonzalez Lopez, S. Goy Lopez, J.M. Hernandez, M.I. Josa, G. Merino, E. Navarro De Martino, J. Puerta Pelayo, A. Quintario Olmeda, I. Redondo, L. Romero, J. Santaolalla, M.S. Soares, C. Willmott

Universidad Autónoma de Madrid, Madrid, Spain

C. Albajar, J.F. de Trocóniz

Universidad de Oviedo, Oviedo, Spain

H. Brun, J. Cuevas, J. Fernandez Menendez, S. Folgueras, I. Gonzalez Caballero, L. Lloret Iglesias, J. Piedra Gomez

Instituto de Física de Cantabria (IFCA), CSIC-Universidad de Cantabria, Santander, Spain

J.A. Brochero Cifuentes, I.J. Cabrillo, A. Calderon, S.H. Chuang, J. Duarte Campderros, M. Fernandez, G. Gomez, J. Gonzalez Sanchez, A. Graziano, C. Jorda, A. Lopez Virto, J. Marco, R. Marco, C. Martinez Rivero, F. Matorras, F.J. Munoz Sanchez, T. Rodrigo, A.Y. Rodríguez-Marrero, A. Ruiz-Jimeno, L. Scodellaro, I. Vila, R. Vilar Cortabitarte

CERN, European Organization for Nuclear Research, Geneva, Switzerland

D. Abbaneo, E. Auffray, G. Auzinger, M. Bachtis, P. Baillon, A.H. Ball, D. Barney, J. Bendavid, J.F. Benitez, C. Bernet⁸, G. Bianchi, P. Bloch, A. Bocci, A. Bonato, O. Bondu, C. Botta, H. Breuker, T. Camporesi, G. Cerminara, T. Christiansen, J.A. Coarasa Perez, S. Colafranceschi³³, D. d'Enterria, A. Dabrowski, A. De Roeck, S. De Visscher, S. Di Guida, M. Dobson, N. Dupont-Sagorin, A. Elliott-Peisert, J. Eugster, W. Funk, G. Georgiou, M. Giffels, D. Gigi, K. Gill, D. Giordano, M. Girone, M. Giunta, F. Glege, R. Gomez-Reino Garrido, S. Gowdy, R. Guida, J. Hammer, M. Hansen, P. Harris, C. Hartl, B. Hegner, A. Hinzmann, V. Innocente, P. Janot, E. Karavakis, K. Kousouris, K. Krajczar, P. Lecoq, Y.-J. Lee, C. Lourenço, N. Magini, M. Malberti, L. Malgeri, M. Mannelli, L. Masetti, F. Meijers, S. Mersi, E. Meschi, R. Moser, M. Mulders, P. Musella, E. Nesvold, L. Orsini, E. Palencia Cortezon, E. Perez, L. Perrozzi, A. Petrilli, A. Pfeiffer, M. Pierini, M. Pimiä, D. Piparo, M. Plagge, G. Polese, L. Quertenmont, A. Racz, W. Reece, G. Rolandi³⁴, C. Rovelli³⁵, M. Rovere, H. Sakulin, F. Santanastasio, C. Schäfer, C. Schwick, I. Segoni, S. Sekmen, A. Sharma, P. Siegrist, P. Silva, M. Simon, P. Sphicas³⁶, D. Spiga, M. Stoye, A. Tsiros, G.I. Veres²¹, J.R. Vlimant, H.K. Wöhri, S.D. Worm³⁷, W.D. Zeuner

Paul Scherrer Institut, Villigen, Switzerland

W. Bertl, K. Deiters, W. Erdmann, K. Gabathuler, R. Horisberger, Q. Ingram, H.C. Kaestli, S. König, D. Kotlinski, U. Langenegger, D. Renker, T. Rohe

Institute for Particle Physics, ETH Zurich, Zurich, Switzerland

F. Bachmair, L. Bäni, P. Bortignon, M.A. Buchmann, B. Casal, N. Chanon, A. Deisher, G. Dissertori, M. Dittmar, M. Donegà, M. Dünser, P. Eller, K. Freudenreich, C. Grab, D. Hits,

P. Lecomte, W. Lustermann, A.C. Marini, P. Martinez Ruiz del Arbol, N. Mohr, F. Moortgat, C. Nägeli³⁸, P. Nef, F. Nessi-Tedaldi, F. Pandolfi, L. Pape, F. Pauss, M. Peruzzi, F.J. Ronga, M. Rossini, L. Sala, A.K. Sanchez, A. Starodumov³⁹, B. Stieger, M. Takahashi, L. Tauscher[†], A. Thea, K. Theofilatos, D. Treille, C. Urscheler, R. Wallny, H.A. Weber

Universität Zürich, Zurich, Switzerland

C. Amsler⁴⁰, V. Chiochia, C. Favaro, M. Ivova Rikova, B. Kilminster, B. Millan Mejias, P. Otiougova, P. Robmann, H. Snoek, S. Taroni, S. Tupputi, M. Verzetti

National Central University, Chung-Li, Taiwan

M. Cardaci, K.H. Chen, C. Ferro, C.M. Kuo, S.W. Li, W. Lin, Y.J. Lu, R. Volpe, S.S. Yu

National Taiwan University (NTU), Taipei, Taiwan

P. Bartalini, P. Chang, Y.H. Chang, Y.W. Chang, Y. Chao, K.F. Chen, C. Dietz, U. Grundler, W.-S. Hou, Y. Hsiung, K.Y. Kao, Y.J. Lei, R.-S. Lu, D. Majumder, E. Petrakou, X. Shi, J.G. Shiu, Y.M. Tzeng, M. Wang

Chulalongkorn University, Bangkok, Thailand

B. Asavapibhop, N. Suwonjandee

Cukurova University, Adana, Turkey

A. Adiguzel, M.N. Bakirci⁴¹, S. Cerci⁴², C. Dozen, I. Dumanoglu, E. Eskut, S. Girgis, G. Gokbulut, E. Gurpinar, I. Hos, E.E. Kangal, A. Kayis Topaksu, G. Onengut⁴³, K. Ozdemir, S. Ozturk⁴¹, A. Polatoz, K. Sogut⁴⁴, D. Sunar Cerci⁴², B. Tali⁴², H. Topakli⁴¹, M. Vergili

Middle East Technical University, Physics Department, Ankara, Turkey

I.V. Akin, T. Aliev, B. Bilin, S. Bilmis, M. Deniz, H. Gamsizkan, A.M. Guler, G. Karapinar⁴⁵, K. Ocalan, A. Ozpineci, M. Serin, R. Sever, U.E. Surat, M. Yalvac, M. Zeyrek

Bogazici University, Istanbul, Turkey

E. Gülmez, B. Isildak⁴⁶, M. Kaya⁴⁷, O. Kaya⁴⁷, S. Ozkorucuklu⁴⁸, N. Sonmez⁴⁹

Istanbul Technical University, Istanbul, Turkey

H. Bahtiyar⁵⁰, E. Barlas, K. Cankocak, Y.O. Günaydin⁵¹, F.I. Vardarli, M. Yücel

National Scientific Center, Kharkov Institute of Physics and Technology, Kharkov, Ukraine

L. Levchuk, P. Sorokin

University of Bristol, Bristol, United Kingdom

J.J. Brooke, E. Clement, D. Cussans, H. Flacher, R. Frazier, J. Goldstein, M. Grimes, G.P. Heath, H.F. Heath, L. Kreczko, S. Metson, D.M. Newbold³⁷, K. Nirunpong, A. Poll, S. Senkin, V.J. Smith, T. Williams

Rutherford Appleton Laboratory, Didcot, United Kingdom

L. Basso⁵², K.W. Bell, A. Belyaev⁵², C. Brew, R.M. Brown, D.J.A. Cockerill, J.A. Coughlan, K. Harder, S. Harper, J. Jackson, E. Olaiya, D. Petyt, B.C. Radburn-Smith, C.H. Shepherd-Themistocleous, I.R. Tomalin, W.J. Womersley

Imperial College, London, United Kingdom

R. Bainbridge, O. Buchmuller, D. Burton, D. Colling, N. Cripps, M. Cutajar, P. Dauncey, G. Davies, M. Della Negra, W. Ferguson, J. Fulcher, D. Futyan, A. Gilbert, A. Guneratne Bryer, G. Hall, Z. Hatherell, J. Hays, G. Iles, M. Jarvis, G. Karapostoli, M. Kenzie, R. Lane, R. Lucas³⁷, L. Lyons, A.-M. Magnan, J. Marrouche, B. Mathias, R. Nandi, J. Nash, A. Nikitenko³⁹, J. Pela, M. Pesaresi, K. Petridis, M. Pioppi⁵³, D.M. Raymond, S. Rogerson, A. Rose, C. Seez, P. Sharp[†], A. Sparrow, A. Tapper, M. Vazquez Acosta, T. Virdee, S. Wakefield, N. Wardle, T. Whyntie

Brunel University, Uxbridge, United Kingdom

M. Chadwick, J.E. Cole, P.R. Hobson, A. Khan, P. Kyberd, D. Leggat, D. Leslie, W. Martin, I.D. Reid, P. Symonds, L. Teodorescu, M. Turner

Baylor University, Waco, USA

J. Dittmann, K. Hatakeyama, A. Kasmi, H. Liu, T. Scarborough

The University of Alabama, Tuscaloosa, USA

O. Charaf, S.I. Cooper, C. Henderson, P. Rumerio

Boston University, Boston, USA

A. Avetisyan, T. Bose, C. Fantasia, A. Heister, P. Lawson, D. Lazic, J. Rohlf, D. Sperka, J. St. John, L. Sulak

Brown University, Providence, USA

J. Alimena, S. Bhattacharya, G. Christopher, D. Cutts, Z. Demiragli, A. Ferapontov, A. Garabedian, U. Heintz, G. Kukartsev, E. Laird, G. Landsberg, M. Luk, M. Narain, M. Segala, T. Sinthuprasith, T. Speer

University of California, Davis, Davis, USA

R. Breedon, G. Breto, M. Calderon De La Barca Sanchez, S. Chauhan, M. Chertok, J. Conway, R. Conway, P.T. Cox, R. Erbacher, M. Gardner, R. Houtz, W. Ko, A. Kopecky, R. Lander, O. Mall, T. Miceli, R. Nelson, D. Pellett, F. Ricci-Tam, B. Rutherford, M. Searle, J. Smith, M. Squires, M. Tripathi, S. Wilbur, R. Yohay

University of California, Los Angeles, USA

V. Andreev, D. Cline, R. Cousins, S. Erhan, P. Everaerts, C. Farrell, M. Felcini, J. Hauser, M. Ignatenko, C. Jarvis, G. Rakness, P. Schlein[†], E. Takasugi, P. Traczyk, V. Valuev, M. Weber

University of California, Riverside, Riverside, USA

J. Babb, R. Clare, M.E. Dinardo, J. Ellison, J.W. Gary, G. Hanson, H. Liu, O.R. Long, A. Luthra, H. Nguyen, S. Paramesvaran, J. Sturdy, S. Sumowidagdo, R. Wilken, S. Wimpenny

University of California, San Diego, La Jolla, USA

W. Andrews, J.G. Branson, G.B. Cerati, S. Cittolin, D. Evans, A. Holzner, R. Kelley, M. Lebourgeois, J. Letts, I. Macneill, B. Mangano, S. Padhi, C. Palmer, G. Petrucciani, M. Pieri, M. Sani, V. Sharma, S. Simon, E. Sudano, M. Tadel, Y. Tu, A. Vartak, S. Wasserbaech⁵⁴, F. Würthwein, A. Yagil, J. Yoo

University of California, Santa Barbara, Santa Barbara, USA

D. Barge, R. Bellan, C. Campagnari, M. D'Alfonso, T. Danielson, K. Flowers, P. Geffert, C. George, F. Golf, J. Incandela, C. Justus, P. Kalavase, D. Kovalskyi, V. Krutelyov, S. Lowette, R. Magaña Villalba, N. Mccoll, V. Pavlunin, J. Ribnik, J. Richman, R. Rossin, D. Stuart, W. To, C. West

California Institute of Technology, Pasadena, USA

A. Apresyan, A. Bornheim, J. Bunn, Y. Chen, E. Di Marco, J. Duarte, D. Kcira, Y. Ma, A. Mott, H.B. Newman, C. Rogan, M. Spiropulu, V. Timciuc, J. Veverka, R. Wilkinson, S. Xie, Y. Yang, R.Y. Zhu

Carnegie Mellon University, Pittsburgh, USA

V. Azzolini, A. Calamba, R. Carroll, T. Ferguson, Y. Iiyama, D.W. Jang, Y.F. Liu, M. Paulini, J. Russ, H. Vogel, I. Vorobiev

University of Colorado at Boulder, Boulder, USA

J.P. Cumalat, B.R. Drell, W.T. Ford, A. Gaz, E. Luiggi Lopez, U. Nauenberg, J.G. Smith, K. Stenson, K.A. Ulmer, S.R. Wagner

Cornell University, Ithaca, USA

J. Alexander, A. Chatterjee, N. Eggert, L.K. Gibbons, W. Hopkins, A. Khukhunaishvili, B. Kreis, N. Mirman, G. Nicolas Kaufman, J.R. Patterson, A. Ryd, E. Salvati, W. Sun, W.D. Teo, J. Thom, J. Thompson, J. Tucker, Y. Weng, L. Winstrom, P. Wittich

Fairfield University, Fairfield, USA

D. Winn

Fermi National Accelerator Laboratory, Batavia, USA

S. Abdullin, M. Albrow, J. Anderson, G. Apollinari, L.A.T. Bauerdick, A. Beretvas, J. Berryhill, P.C. Bhat, K. Burkett, J.N. Butler, V. Chetluru, H.W.K. Cheung, F. Chlebana, S. Cihangir, V.D. Elvira, I. Fisk, J. Freeman, Y. Gao, E. Gottschalk, L. Gray, D. Green, O. Gutsche, D. Hare, R.M. Harris, J. Hirschauer, B. Hooberman, S. Jindariani, M. Johnson, U. Joshi, B. Klima, S. Kunori, S. Kwan, C. Leonidopoulos⁵⁵, J. Linacre, D. Lincoln, R. Lipton, J. Lykken, K. Maeshima, J.M. Marraffino, V.I. Martinez Outschoorn, S. Maruyama, D. Mason, P. McBride, K. Mishra, S. Mrenna, Y. Musienko⁵⁶, C. Newman-Holmes, V. O'Dell, O. Prokofyev, N. Ratnikova, E. Sexton-Kennedy, S. Sharma, W.J. Spalding, L. Spiegel, L. Taylor, S. Tkaczyk, N.V. Tran, L. Uplegger, E.W. Vaandering, R. Vidal, J. Whitmore, W. Wu, F. Yang, J.C. Yun

University of Florida, Gainesville, USA

D. Acosta, P. Avery, D. Bourilkov, M. Chen, T. Cheng, S. Das, M. De Gruttola, G.P. Di Giovanni, D. Dobur, A. Drozdetskiy, R.D. Field, M. Fisher, Y. Fu, I.K. Furic, J. Hugon, B. Kim, J. Konigsberg, A. Korytov, A. Kropivnitskaya, T. Kypreos, J.F. Low, K. Matchev, P. Milenovic⁵⁷, G. Mitselmakher, L. Muniz, R. Remington, A. Rinkevicius, N. Skhirtladze, M. Snowball, J. Yelton, M. Zakaria

Florida International University, Miami, USA

V. Gaultney, S. Hewamanage, L.M. Lebolo, S. Linn, P. Markowitz, G. Martinez, J.L. Rodriguez

Florida State University, Tallahassee, USA

T. Adams, A. Askew, J. Bochenek, J. Chen, B. Diamond, S.V. Gleyzer, J. Haas, S. Hagopian, V. Hagopian, K.F. Johnson, H. Prosper, V. Veeraraghavan, M. Weinberg

Florida Institute of Technology, Melbourne, USA

M.M. Baarmand, B. Dorney, M. Hohlmann, H. Kalakhety, F. Yumiceva

University of Illinois at Chicago (UIC), Chicago, USA

M.R. Adams, L. Apanasevich, V.E. Bazterra, R.R. Betts, I. Bucinskaite, J. Callner, R. Cavanaugh, O. Evdokimov, L. Gauthier, C.E. Gerber, D.J. Hofman, S. Khalatyan, P. Kurt, F. Lacroix, D.H. Moon, C. O'Brien, C. Silkworth, D. Strom, P. Turner, N. Varelas

The University of Iowa, Iowa City, USA

U. Akgun, E.A. Albayrak⁵⁰, B. Bilki⁵⁸, W. Clarida, K. Dilsiz, F. Duru, S. Griffiths, J.-P. Merlo, H. Mermerkaya⁵⁹, A. Mestvirishvili, A. Moeller, J. Nachtman, C.R. Newsom, H. Ogul, Y. Onel, F. Ozok⁵⁰, S. Sen, P. Tan, E. Tiras, J. Wetzel, T. Yetkin⁶⁰, K. Yi

Johns Hopkins University, Baltimore, USA

B.A. Barnett, B. Blumenfeld, S. Bolognesi, D. Fehling, G. Giurgiu, A.V. Gritsan, Z.J. Guo, G. Hu, P. Maksimovic, M. Swartz, A. Whitbeck

The University of Kansas, Lawrence, USA

P. Baringer, A. Bean, G. Benelli, R.P. Kenny III, M. Murray, D. Noonan, S. Sanders, R. Stringer, J.S. Wood

Kansas State University, Manhattan, USA

A.F. Barfuss, I. Chakaberia, A. Ivanov, S. Khalil, M. Makouski, Y. Maravin, S. Shrestha, I. Svintradze

Lawrence Livermore National Laboratory, Livermore, USA

J. Gronberg, D. Lange, F. Rebassoo, D. Wright

University of Maryland, College Park, USA

A. Baden, B. Calvert, S.C. Eno, J.A. Gomez, N.J. Hadley, R.G. Kellogg, T. Kolberg, Y. Lu, M. Marionneau, A.C. Mignerey, K. Pedro, A. Peterman, A. Skuja, J. Temple, M.B. Tonjes, S.C. Tonwar

Massachusetts Institute of Technology, Cambridge, USA

A. Apyan, G. Bauer, W. Busza, E. Butz, I.A. Cali, M. Chan, V. Dutta, G. Gomez Ceballos, M. Goncharov, Y. Kim, M. Klute, Y.S. Lai, A. Levin, P.D. Luckey, T. Ma, S. Nahn, C. Paus, D. Ralph, C. Roland, G. Roland, G.S.F. Stephans, F. Stöckli, K. Sumorok, K. Sung, D. Velicanu, R. Wolf, B. Wyslouch, M. Yang, Y. Yilmaz, A.S. Yoon, M. Zanetti, V. Zhukova

University of Minnesota, Minneapolis, USA

B. Dahmes, A. De Benedetti, G. Franzoni, A. Gude, J. Haupt, S.C. Kao, K. Klapoetke, Y. Kubota, J. Mans, N. Pastika, R. Rusack, M. Sasseville, A. Singovsky, N. Tambe, J. Turkewitz

University of Mississippi, Oxford, USA

L.M. Cremaldi, R. Kroeger, L. Perera, R. Rahmat, D.A. Sanders, D. Summers

University of Nebraska-Lincoln, Lincoln, USA

E. Avdeeva, K. Bloom, S. Bose, D.R. Claes, A. Dominguez, M. Eads, R. Gonzalez Suarez, J. Keller, I. Kravchenko, J. Lazo-Flores, S. Malik, F. Meier, G.R. Snow

State University of New York at Buffalo, Buffalo, USA

J. Dolen, A. Godshalk, I. Iashvili, S. Jain, A. Kharchilava, A. Kumar, S. Rappoccio, Z. Wan

Northeastern University, Boston, USA

G. Alverson, E. Barberis, D. Baumgartel, M. Chasco, J. Haley, D. Nash, T. Orimoto, D. Trocino, D. Wood, J. Zhang

Northwestern University, Evanston, USA

A. Anastassov, K.A. Hahn, A. Kubik, L. Lusito, N. Mucia, N. Odell, B. Pollack, A. Pozdnyakov, M. Schmitt, S. Stoynev, M. Velasco, S. Won

University of Notre Dame, Notre Dame, USA

D. Berry, A. Brinkerhoff, K.M. Chan, M. Hildreth, C. Jessop, D.J. Karmgard, J. Kolb, K. Lannon, W. Luo, S. Lynch, N. Marinelli, D.M. Morse, T. Pearson, M. Planer, R. Ruchti, J. Slaunwhite, N. Valls, M. Wayne, M. Wolf

The Ohio State University, Columbus, USA

L. Antonelli, B. Bylsma, L.S. Durkin, C. Hill, R. Hughes, K. Kotov, T.Y. Ling, D. Puigh, M. Rodenburg, G. Smith, C. Vuosalo, G. Williams, B.L. Winer, H. Wolfe

Princeton University, Princeton, USA

E. Berry, P. Elmer, V. Halyo, P. Hebda, J. Hegeman, A. Hunt, P. Jindal, S.A. Koay, D. Lopes

Pegna, P. Lujan, D. Marlow, T. Medvedeva, M. Mooney, J. Olsen, P. Piroué, X. Quan, A. Raval, H. Saka, D. Stickland, C. Tully, J.S. Werner, S.C. Zenz, A. Zuranski

University of Puerto Rico, Mayaguez, USA

E. Brownson, A. Lopez, H. Mendez, J.E. Ramirez Vargas

Purdue University, West Lafayette, USA

E. Alagoz, D. Benedetti, G. Bolla, D. Bortoletto, M. De Mattia, A. Everett, Z. Hu, M. Jones, K. Jung, O. Koybasi, M. Kress, N. Leonardo, V. Maroussov, P. Merkel, D.H. Miller, N. Neumeister, I. Shipsey, D. Silvers, A. Svyatkovskiy, M. Vidal Marono, F. Wang, L. Xu, H.D. Yoo, J. Zablocki, Y. Zheng

Purdue University Calumet, Hammond, USA

S. Guragain, N. Parashar

Rice University, Houston, USA

A. Adair, B. Akgun, K.M. Ecklund, F.J.M. Geurts, W. Li, B.P. Padley, R. Redjimi, J. Roberts, J. Zabel

University of Rochester, Rochester, USA

B. Betchart, A. Bodek, R. Covarelli, P. de Barbaro, R. Demina, Y. Eshaq, T. Ferbel, A. Garcia-Bellido, P. Goldenzweig, J. Han, A. Harel, D.C. Miner, G. Petrillo, D. Vishnevskiy, M. Zielinski

The Rockefeller University, New York, USA

A. Bhatti, R. Ciesielski, L. Demortier, K. Goulianos, G. Lungu, S. Malik, C. Mesropian

Rutgers, The State University of New Jersey, Piscataway, USA

S. Arora, A. Barker, J.P. Chou, C. Contreras-Campana, E. Contreras-Campana, D. Duggan, D. Ferencek, Y. Gershtein, R. Gray, E. Halkiadakis, D. Hidas, A. Lath, S. Panwalkar, M. Park, R. Patel, V. Rekovic, J. Robles, K. Rose, S. Salur, S. Schnetzer, C. Seitz, S. Somalwar, R. Stone, S. Thomas, M. Walker

University of Tennessee, Knoxville, USA

G. Cerizza, M. Hollingsworth, S. Spanier, Z.C. Yang, A. York

Texas A&M University, College Station, USA

R. Eusebi, W. Flanagan, J. Gilmore, T. Kamon⁶¹, V. Khotilovich, R. Montalvo, I. Osipenkov, Y. Pakhotin, A. Perloff, J. Roe, A. Safonov, T. Sakuma, I. Suarez, A. Tatarinov, D. Toback

Texas Tech University, Lubbock, USA

N. Akchurin, J. Damgov, C. Dragoiu, P.R. Duderu, C. Jeong, K. Kovitangoon, S.W. Lee, T. Libeiro, I. Volobouev

Vanderbilt University, Nashville, USA

E. Appelt, A.G. Delannoy, S. Greene, A. Gurrola, W. Johns, C. Maguire, Y. Mao, A. Melo, M. Sharma, P. Sheldon, B. Snook, S. Tuo, J. Velkovska

University of Virginia, Charlottesville, USA

M.W. Arenton, S. Boutle, B. Cox, B. Francis, J. Goodell, R. Hirosky, A. Ledovskoy, C. Lin, C. Neu, J. Wood

Wayne State University, Detroit, USA

S. Gollapinni, R. Harr, P.E. Karchin, C. Kottachchi Kankanamge Don, P. Lamichhane, A. Sakharov

University of Wisconsin, Madison, USA

M. Anderson, D.A. Belknap, L. Borrello, D. Carlsmith, M. Cepeda, S. Dasu, E. Friis, K.S. Grogg, M. Grothe, R. Hall-Wilton, M. Herndon, A. Hervé, K. Kaadze, P. Klabbers, J. Klukas, A. Lanaro, C. Lazaridis, R. Loveless, A. Mohapatra, M.U. Mozer, I. Ojalvo, G.A. Pierro, I. Ross, A. Savin, W.H. Smith, J. Swanson

†: Deceased

- 1: Also at Vienna University of Technology, Vienna, Austria
- 2: Also at CERN, European Organization for Nuclear Research, Geneva, Switzerland
- 3: Also at Institut Pluridisciplinaire Hubert Curien, Université de Strasbourg, Université de Haute Alsace Mulhouse, CNRS/IN2P3, Strasbourg, France
- 4: Also at National Institute of Chemical Physics and Biophysics, Tallinn, Estonia
- 5: Also at Skobeltsyn Institute of Nuclear Physics, Lomonosov Moscow State University, Moscow, Russia
- 6: Also at Universidade Estadual de Campinas, Campinas, Brazil
- 7: Also at California Institute of Technology, Pasadena, USA
- 8: Also at Laboratoire Leprince-Ringuet, Ecole Polytechnique, IN2P3-CNRS, Palaiseau, France
- 9: Also at Suez Canal University, Suez, Egypt
- 10: Also at Cairo University, Cairo, Egypt
- 11: Also at Fayoum University, El-Fayoum, Egypt
- 12: Also at Helwan University, Cairo, Egypt
- 13: Also at British University in Egypt, Cairo, Egypt
- 14: Now at Ain Shams University, Cairo, Egypt
- 15: Also at National Centre for Nuclear Research, Swierk, Poland
- 16: Also at Université de Haute Alsace, Mulhouse, France
- 17: Also at Joint Institute for Nuclear Research, Dubna, Russia
- 18: Also at Brandenburg University of Technology, Cottbus, Germany
- 19: Also at The University of Kansas, Lawrence, USA
- 20: Also at Institute of Nuclear Research ATOMKI, Debrecen, Hungary
- 21: Also at Eötvös Loránd University, Budapest, Hungary
- 22: Also at Tata Institute of Fundamental Research - HECR, Mumbai, India
- 23: Now at King Abdulaziz University, Jeddah, Saudi Arabia
- 24: Also at University of Visva-Bharati, Santiniketan, India
- 25: Also at University of Ruhuna, Matara, Sri Lanka
- 26: Also at Sharif University of Technology, Tehran, Iran
- 27: Also at Isfahan University of Technology, Isfahan, Iran
- 28: Also at Plasma Physics Research Center, Science and Research Branch, Islamic Azad University, Tehran, Iran
- 29: Also at Laboratori Nazionali di Legnaro dell' INFN, Legnaro, Italy
- 30: Also at Università degli Studi di Siena, Siena, Italy
- 31: Also at Universidad Michoacana de San Nicolas de Hidalgo, Morelia, Mexico
- 32: Also at Faculty of Physics, University of Belgrade, Belgrade, Serbia
- 33: Also at Facoltà Ingegneria, Università di Roma, Roma, Italy
- 34: Also at Scuola Normale e Sezione dell'INFN, Pisa, Italy
- 35: Also at INFN Sezione di Roma, Roma, Italy
- 36: Also at University of Athens, Athens, Greece
- 37: Also at Rutherford Appleton Laboratory, Didcot, United Kingdom
- 38: Also at Paul Scherrer Institut, Villigen, Switzerland
- 39: Also at Institute for Theoretical and Experimental Physics, Moscow, Russia
- 40: Also at Albert Einstein Center for Fundamental Physics, Bern, Switzerland

-
- 41: Also at Gaziosmanpasa University, Tokat, Turkey
 - 42: Also at Adiyaman University, Adiyaman, Turkey
 - 43: Also at Cag University, Mersin, Turkey
 - 44: Also at Mersin University, Mersin, Turkey
 - 45: Also at Izmir Institute of Technology, Izmir, Turkey
 - 46: Also at Ozyegin University, Istanbul, Turkey
 - 47: Also at Kafkas University, Kars, Turkey
 - 48: Also at Suleyman Demirel University, Isparta, Turkey
 - 49: Also at Ege University, Izmir, Turkey
 - 50: Also at Mimar Sinan University, Istanbul, Istanbul, Turkey
 - 51: Also at Kahramanmaras Sütcü Imam University, Kahramanmaras, Turkey
 - 52: Also at School of Physics and Astronomy, University of Southampton, Southampton, United Kingdom
 - 53: Also at INFN Sezione di Perugia; Università di Perugia, Perugia, Italy
 - 54: Also at Utah Valley University, Orem, USA
 - 55: Now at University of Edinburgh, Scotland, Edinburgh, United Kingdom
 - 56: Also at Institute for Nuclear Research, Moscow, Russia
 - 57: Also at University of Belgrade, Faculty of Physics and Vinca Institute of Nuclear Sciences, Belgrade, Serbia
 - 58: Also at Argonne National Laboratory, Argonne, USA
 - 59: Also at Erzincan University, Erzincan, Turkey
 - 60: Also at Yildiz Technical University, Istanbul, Turkey
 - 61: Also at Kyungpook National University, Daegu, Korea